Fast Calibration for Computer Models with Massive Physical Observations

Shurui Lv*

School of Statistics and Data Science, Faculty of Science, Beijing
University of Technology, Beijing, China
Yan Wang
School of Statistics and Data Science, Faculty of Science, Beijing
University of Technology, Beijing, China
and
Jun Yu
School of Mathematics and Statistics, Beijing Institute of Technology,
Beijing 100081, China

November 24, 2022

Abstract

Computer model calibration is a crucial step in building a reliable computer model. In the face of massive physical observations, a fast estimation for the calibration parameters is urgently needed. To alleviate the computational burden, we design a two-step algorithm to estimate the calibration parameters by employing the subsampling techniques. Compared with the current state-of-the-art calibration methods, the complexity of the proposed algorithm is greatly reduced without sacrificing too much accuracy. We prove the consistency and asymptotic normality of the proposed estimator. The form of the variance of the proposed estimation is also presented, which provides a natural way to quantify the uncertainty of the calibration parameters. The obtained results of two numerical simulations and two real-case studies demonstrate the advantages of the proposed method.

Keywords: Massive Data, Weighted Least Squares Calibration, Optimal Subsampling, Poisson Sampling

---

*Correspondence should be addressed to Yan Wang (yanwang@bjut.edu.cn)

1

1 Introduction

Computer models, or simulators, are being used increasingly to mimic complex systems in physics, engineering, and human processes. A computer model usually involves additional model parameters that cannot be determined or observed in physical processes. Tuning these parameters is essential to match the computer outputs with the physical observations. The corresponding stage is called the *calibration* of computer models, and the parameters are usually referred as *calibration parameters*.

Several methods have been established to estimate the calibration parameters, such as the KO's calibration (Kennedy and O'Hagan, 2001), L_2 calibration (Tuo and Wu, 2015), ordinary least squares (OLS) calibration (Wong et al., 2017), orthogonal Gaussian Process (GP) model calibration (Plumlee, 2017), projected kernel calibration (Tuo, 2019), and Bayesian projected calibration (Xie and Xu, 2021).

Despite the great success achieved by the aforementioned methods, the computational complexity of those methods is greater than or equal to $O(n^2)$, where n is the sample size of the physical observations. Consequently, there is an urgent need to develop a fast calibration method for dealing with the case that the available physical observations are massive, which is common in many calibration problems. For example, in the calibration of a traffic flow model (Hou et al., 2013), more than $30,000$ actual traffic data per year were collected by one detector in the UK's M25 freeway. All the detectors in the UK's M25 freeway can collect more than 10 million data per year (http://tris.highwaysengland.co.uk/detail/trafficflowdata).

Besides the common two computational barriers for general big data analysis: (1) data is too large to be held in a computer's memory; and (2) computation by using whole physical observations is time-consuming in obtaining the estimated results. The calibration with

massive physical observations meets additional challenge since that the computer models are always expensive. To be precise, the computer outputs at all the physical observation points are needed to evaluate how well they match the real physical observations. It is time-consuming to run computer models at all the physical observations. Although cheaper surrogate models can be built to mimic the computer outputs (Santner et al., 2018), it may still be unaffordable to predict the computer outputs at all the physical observations.

To address these computational barriers, the parallel computing method has been successfully applied to the calibration for computer models, see Cai and Mahadevan (2017); Chang and Guillas (2019); Tsai et al. (2021) and the references therein. These methods improve computational efficiency by dividing the whole data set into subsets, estimating the calibration parameters with the subsets at the same time, and combining the results from subsets to obtain a final estimator. However, such a method is still expensive since it naturally requires more computational resources. Moreover, debugging is certainly easier and faster with fewer observations. Besides parallel computing, another well-known tool to reduce the computational burden is subsampling. The core of the subsampling method is to use non-uniform subsampling probabilities to include data points into the subsamples with a larger probability. It is worth mentioning that most of the current subsampling strategies focus on the specified regression models (Mahoney et al., 2015; Wang et al., 2019; Zhu, 2016; Wang et al., 2018; Yao and Wang, 2019; Wang and Ma, 2021; Ai et al., 2021; Yu et al., 2022), where the regression model is a specified function on the parameters to be estimated. However, in general, the computer models to be calibrated are difficult to be represented as a specified function of the calibration parameters. The existing subsampling methods can not be directly applied to the calibration for the computer models.

Nevertheless, the idea of subsampling is valuable to help researchers efficiently down-

size the data volume and naturally accelerate the downstreaming analysis. Similar to the existing subsampling literature, this work aims to select subsamples that contain more information about calibration parameters and derive a fast estimator based on the selected subsamples. The contributions of this work include the following:

- We propose an inverse probability weighted least squares (IPWLS) calibration method using subsamples obtained based on the optimal subsampling probabilities. A practical two-step algorithm is also given to approximate the IPWLS estimator with theoretical backups.

- Compared to the existing lowest computational complexity method which is the OLS calibration, the proposed calibration method is computational more efficient.

- The proposed estimator is proven to be consistent and asymptotically normal. Based on the asymptotic variance, a formula for the standard error of the proposed estimator is derived, which provides a natural way for the uncertainty quantification of the calibration parameters.

The remainder of this work is organized as follows. Section 2 gives a brief review of the OLS calibration for computer models, which has the lowest computational complexity among the existing calibration methods. In Section 3, we introduce an IPWLS calibration based on the OLS calibration. We prove the asymptotic properties of the proposed estimator based on subsamples and derive the optimal subsampling probabilities based on A- and L-optimality criteria. In Section 4, a practical two-step algorithm is proposed to approximate the proposed estimator. The asymptotic results and the standard error of the resulting estimator are also presented. Section 5 examines the proposed method through two numerical simulations and two real data studies. Section 6 concludes the paper with some discussion. All technique proofs are deferred in Supplementary Material.

2 Preliminaries

In this section, we give a brief introduction to the OLS calibration (Wong et al., 2017), which enjoys the lowest computational complexity among all the existing calibration methods.

Denote the input domain of physical experiments by $\boldsymbol{\Omega}$, which is assumed to be a convex and compact subset of $\mathbb{R}^d$. Let $\boldsymbol{X} = \{\boldsymbol{x}_1, \ldots, \boldsymbol{x}_n\} \subseteq \boldsymbol{\Omega}$ be the set of design points for the physical experiments and $\boldsymbol{Y}^p = (y_1^p, \ldots, y_n^p)^T$ be the corresponding physical responses, with the superscript p indicating "physical". Suppose the physical experimental observation is generated by

$$y_i^p = \zeta(\boldsymbol{x}_i) + e_i, \ i = 1, \ldots, n, \tag{2.1}$$

where $\zeta(\cdot)$ is an unknown function, called the *true process*; and e_i's are independent and identically distributed random variables with zero mean and finite variance $\sigma^2 > 0$.

Let $\boldsymbol{\theta} \in \boldsymbol{\Theta}$ to be the calibration parameter. Suppose that the parameter space $\boldsymbol{\Theta}$ is a compact subset of $\mathbb{R}^q$. Let $y^s(\boldsymbol{x}, \boldsymbol{\theta})$ be the computer model which is used to simulate the true process $\zeta(\boldsymbol{x})$. Here, the superscript s indicates "simulated". Following from Tuo and Wu (2015) and Wong et al. (2017), the "true" value of calibration parameter is defined as

$$\boldsymbol{\theta}^* := \operatorname*{arg\,min}_{\theta \in \boldsymbol{\Theta}} \int_{\boldsymbol{\Omega}} \left[\zeta(\boldsymbol{x}) - y^s(\boldsymbol{x}, \boldsymbol{\theta}) \right]^2 dF(\boldsymbol{x}), \tag{2.2}$$

where F is the sampling distribution of $\boldsymbol{x}$. The goal of calibration is to estimate $\boldsymbol{\theta}^*$ such that the computer outputs are as close as possible to the physical experimental observations. A natural estimator for $\boldsymbol{\theta}^*$ is the minimizer of the following loss function (Tuo and Wu, 2015)

$$\operatorname*{arg\,min}_{\boldsymbol{\theta} \in \boldsymbol{\Theta}} \frac{1}{n} \sum_{i=1}^{n} \left[y_i^p - y^s(\boldsymbol{x}_i, \boldsymbol{\theta}) \right]^2. \tag{2.3}$$

When the computer model is expensive, only a limited number of computer experiments can be run. It is hard to perform computer experiments at all the physical observation

points. Hence, a surrogate model is needed to mimic the computer outputs. The predictor of the computer model is denoted by $\hat{y}^s(\boldsymbol{x}, \boldsymbol{\theta})$. By plugging $\hat{y}^s(\boldsymbol{x}, \boldsymbol{\theta})$ into (2.3), the OLS estimator can be obtained as follows,

$$\hat{\boldsymbol{\theta}} := \arg\min_{\boldsymbol{\theta} \in \boldsymbol{\Theta}} \frac{1}{n} \sum_{i=1}^{n} [y_i^p - \hat{y}^s(\boldsymbol{x}_i, \boldsymbol{\theta})]^2 . \tag{2.4}$$

By assuming the approximation error of the surrogate model $\hat{y}^s(\cdot, \cdot)$ is negligible, i.e., $\sup_{(\boldsymbol{x}, \boldsymbol{\theta}) \in \boldsymbol{\Omega} \times \boldsymbol{\Theta}} |y^s(\boldsymbol{x}, \boldsymbol{\theta}) - \hat{y}^s(\boldsymbol{x}, \boldsymbol{\theta})| = o_p(n^{-1/2})$, Tuo and Wu (2015) and Wong et al. (2017) proved that the OLS estimator (2.4) converges to the "true" value of the calibration parameter (2.2) with the convergence rate $O_p(n^{-1/2})$ and the OLS estimate is asymptotically normal, i.e., $\hat{\boldsymbol{\theta}} \sim N(\boldsymbol{\theta}^*, \boldsymbol{\Sigma})$ in distribution. Here, $\boldsymbol{\Sigma}$ can be evaluated by

$$\boldsymbol{\Sigma} = \frac{1}{n} \mathbf{J}^{-1} \mathbf{V} \mathbf{J}^{-1}, \tag{2.5}$$

with

$$\mathbf{J} = \int_{\boldsymbol{\Omega}} \frac{\partial^2 [\zeta(\boldsymbol{x}) - y^s(\boldsymbol{x}, \boldsymbol{\theta}^*)]^2}{\partial \boldsymbol{\theta} \partial \boldsymbol{\theta}^T} dF(\boldsymbol{x}), \tag{2.6}$$

and

$$\mathbf{V} = 4 \int_{\boldsymbol{\Omega}} \left\{ [\zeta(\boldsymbol{x}) - y^s(\boldsymbol{x}, \boldsymbol{\theta}^*)]^2 + \sigma^2 \right\} \frac{\partial y^s(\boldsymbol{x}, \boldsymbol{\theta}^*)}{\partial \boldsymbol{\theta}^T} \frac{\partial y^s(\boldsymbol{x}, \boldsymbol{\theta}^*)}{\partial \boldsymbol{\theta}} dF(\boldsymbol{x}). \tag{2.7}$$

From Tuo and Wu (2015), the OLS calibration is less efficient than the L_2 calibration. Specifically, the estimator given by the L_2 calibration method achieves the asymptotic variance with $\boldsymbol{\Sigma}_{opt} = \frac{1}{n} \mathbf{J}^{-1} \mathbf{V}_{opt} \mathbf{J}^{-1}$ and $\mathbf{V}_{opt} = 4\sigma^2 \int_{\boldsymbol{\Omega}} \frac{\partial y^s(\boldsymbol{x}, \boldsymbol{\theta}^*)}{\partial \boldsymbol{\theta}^T} \frac{\partial y^s(\boldsymbol{x}, \boldsymbol{\theta}^*)}{\partial \boldsymbol{\theta}} dF(\boldsymbol{x})$. Since the computer models are built under many assumptions and simplifications the bias between $\zeta(\cdot)$ and $y^s(\cdot, \boldsymbol{\theta}^*)$ can be large in practical situations (Kennedy and O'Hagan, 2001). Suppose $\frac{\partial y^s(\boldsymbol{x}, \boldsymbol{\theta}^*)}{\partial \boldsymbol{\theta}} \neq \mathbf{0}$ for $\boldsymbol{x} \in \boldsymbol{\Omega}$, one can see that $\boldsymbol{\Sigma} - \boldsymbol{\Sigma}_{opt} \geq 0$. This implies that the OLS calibration can lead to a larger variance compared with the L_2 calibration, especially for the scenario that the physical observations are limited. Note that $\boldsymbol{\Sigma} - \boldsymbol{\Sigma}_{opt} = O_p(n^{-1})$. The difference between $\boldsymbol{\Sigma}$ and $\boldsymbol{\Sigma}_{opt}$ is negligible as the physical observations increase. For

the calibration with massive physical observations, the OLS calibration method is still considered as a method that can achieve the highest possible efficiency.

Besides the high efficiency, the OLS estimator is conceptually clean and simple, easy to understand and calculate (Wong et al., 2017). For an expensive computer model, suppose a GP model (Santner et al., 2018) is built as the surrogate by using m computer experiments, the computational complexities of building the GP model and predicting the computer outputs at $\{(\boldsymbol{x}_i^T, \boldsymbol{\theta}^T)^T\}_{i=1}^n$ are $O(m^3)$ and $O(nm)$, respectively. Assume that the asymptotic step of finding the optimal solution of (2.4) is w_n. For example, suppose the gradient descent method is adopted to query the optimal solution of (2.4), then $w_n = O(\log(n))$ (Bottou, 2010). With each iteration, we need to recalculate the gradient of the empirical loss (2.4) and re-predict the computer outputs at $\{(\boldsymbol{x}_i^T, \boldsymbol{\theta}^T)^T\}_{i=1}^n$. That is, the computational complexity of the OLS calibration is $O(w_n n q^2 + w_n nm + m^3)$. It is at least $O(n^3)$ lower than that of the other existing calibration methods because the computations of the other existing calibration methods involve the inverse of a covariance matrix of n by n.

Although the OLS calibration method enjoys these advantages, the computational problems are still the biggest snag when the physical observations are massive. Even if we ignore the computing time to build the emulator for y^s and to predict the computer outputs at the physical observation points, the computational complexity of the OLS calibration is still $O(w_n n q^2)$. Thus, a fast calibration method is needed to reduce the computational burden.

3   Calibration via Subsampling

To reduce the computational complexity, we introduce a fast estimator by using general Poisson subsampling method. We prove that the proposed estimate can effectively approximate the true value of the calibration parameter (2.2). We also derive the optimal

subsampling probabilities in the sense that the resulting estimate achieves the minimizing asymptotic mean square error (MSE).

3.1 IPWLS Calibration

Let π_i to be the probability to sample the i-th data point for $i = 1, \ldots, n$. Let $S = \{(\boldsymbol{x}_i^{*T}, y^p(\boldsymbol{x}_i^*), \pi_i)^T\}_{i=1}^r$ be a set of subsamples and the corresponding sampling probabilities. To improve computational efficiency, a novel calibration method can be constructed by using the subsample set S to approximate the full data OLS estimates. Inspired by sampling theory, we suggest an inverse probability weighted least squares estimator, denoted as *IPWLS* estimate, by solving the following minimization problem

$$\tilde{\boldsymbol{\theta}} := \arg\min_{\boldsymbol{\theta} \in \boldsymbol{\Theta}} l^*(\boldsymbol{\theta}), \tag{3.1}$$

where

$$l^*(\boldsymbol{\theta}) = \frac{1}{n} \sum_{i=1}^r \frac{1}{\pi_i} \left[y^p(\boldsymbol{x}_i^*) - \hat{y}^s(\boldsymbol{x}_i^*, \boldsymbol{\theta}) \right]^2. \tag{3.2}$$

It can be seen that, with given subsample set S, the computer outputs need to be predicted only at the locations of the r subsamples. Let the asymptotic number of iterations for optimizing (3.2) is w_r. For given sampling probabilities, the computational complexity of the proposed estimator is $O(w_r r q^2 + w_r r m + m^3)$. By assuming $r \ll n$, which is natural in the big data setting, this method can drastically reduce the computational complexity.

Now, we focus on the choice of the subsamples. As subsampling with replacement according to unequal probabilities requires accessing subsampling probabilities for the full data all at once. This takes a large memory to implement and may reduce the computational efficiency. To overcome this challenge, we apply the Poisson sampling (Yu et al., 2022) to generate subsamples. The general IPWLS calibration based on the Poisson sampling is shown in Algorithm 1.

Algorithm 1: General IPWLS calibration

Initialization: $S = \varnothing$;

for $i = 1, ..., n$ **do**

    Generate a Bernoulli variable $a_i \sim B(1, \pi_i)$;

    if $a_i = 1$ **then**

        Update $S = S \cup \{(\boldsymbol{x}_i, y_i^p, \pi_i)\}$;

    else

        $S = S$.

end

Estimation: Obtain $\tilde{\boldsymbol{\theta}}$ (3.1) based on the subsample set S.

Remark 3.1. *The subsample size, say r^*, in Algorithm 1 is random such that $E(r^*) = \sum_{i=1}^{n} \pi_i$. We use $r = \sum_{i=1}^{n} \pi_i$ to denote the expected subsample size. As shown in Ai et al. (2021) that r is still concentrated around its expectation with a high probability, the sampling budget is still under control.*

From Algorithm 1, we can see that each π_i can be calculated for each individual data point when scanning the full data. It can save computer memory effectively. Accordingly, the proposed calibration method addresses the three computational barriers faced by massive data calibration as mentioned in Section 1.

Suppose the predictor $\hat{y}^s(\cdot, \cdot)$ is built by using the computer experimental data $\mathcal{D}^s = \{(\boldsymbol{x}_i^s, \boldsymbol{\theta}_i^s); y_i^s\}_{i=1}^{m}$. Following Ezzat et al. (2018), we generate computer experimental design points independently of the physical observation points. The accuracy of the predictor $\hat{y}^s(\cdot, \cdot)$ is independent on the physical observations and it is not required to be considered in the subsampling process.

3.2 Asymptotic Properties

Denote the full physical data as $\mathcal{D}_n = \{(\boldsymbol{x}_i, y_i^p)\}_{i=1}^n$. Assume the physical design points $\{\boldsymbol{x}_i\}_{i=1}^n$ are fixed and use F_n to denote their empirical distribution. For two functions f_1 and f_2, let $\|\cdot\|_n$ represents the $L_2(F_n)-$ norm, with $<f_1, f_2>_n = \frac{1}{n}\sum_{i=1}^n f_1(\boldsymbol{x}_i)f_2(\boldsymbol{x}_i)$ and $\|\cdot\|$ represents the $L_2(F)-$ norm with $<f_1, f_2> = \int_{\boldsymbol{\Omega}} f_1(\boldsymbol{x})f_2(\boldsymbol{x})dF(\boldsymbol{x})$. Let $\|\cdot\|_E$ to be the Euclidean norm, and $\|f_1\|_{L_\infty(\boldsymbol{\Omega})} = \sup_{\boldsymbol{x}\in\boldsymbol{\Omega}} f_1(\boldsymbol{x})$. Next, we discuss the asymptotic properties of $\tilde{\boldsymbol{\theta}}$. The approximating error of the predictor $\hat{y}^s(\cdot,\cdot)$ can be well-controlled by carefully selected design (Haaland et al., 2018) and moderate amount of computer experiments. As suggested in Tuo and Wu (2015) and Wong et al. (2017), we ignore the uncertainty of $\hat{y}^s(\cdot,\cdot)$ in this work by assuming that $\|\hat{y}^s - y^s\|_{L_\infty(\boldsymbol{\Omega}\times\boldsymbol{\Theta})} = o_p(n^{-1/2})$.

Now, let us list the necessary assumptions for obtaining convergence results.

(H.1) $\{e_i\}$ is a sequence of i.i.d. random variables with zero mean and finite variance. Also, assume that $\mathrm{E}e_i^6 < \infty$.

(H.2) $\boldsymbol{\theta}^*$ is the unique solution to (2.2), and an interior point of $\boldsymbol{\Theta}$.

(H.3) Suppose the design $\boldsymbol{X}$ satisfies that

    (i) $\sup_{\boldsymbol{\theta}\in\boldsymbol{\Theta}} |\|\zeta - y^s(\cdot,\boldsymbol{\theta})\|_n^2 - \|\zeta - y^s(\cdot,\boldsymbol{\theta})\|^2| = o_p(1)$;

    (ii) Elements of $\mathbf{J}_n - \mathbf{J}$ are $o_p(1)$, where $\mathbf{J}$ is defined in (2.6) and

$$\mathbf{J}_n = \frac{1}{n}\sum_{i=1}^n \frac{\partial^2[\zeta(\boldsymbol{x}_i) - y^s(\boldsymbol{x}_i, \boldsymbol{\theta}^*)]^2}{\partial\boldsymbol{\theta}\partial\boldsymbol{\theta}^T}; \tag{3.3}$$

    (iii) $\frac{1}{n}\sum_{i=1}^n \frac{\partial[\zeta(\boldsymbol{x}_i) - y^s(\boldsymbol{x}_i, \boldsymbol{\theta}^*)]^2}{\partial\boldsymbol{\theta}} = O_p(n^{-1/2})$.

(H.4) Assume $\lambda_{\min}(\mathbf{J}) > 0$ and $\lambda_{\max}(\mathbf{J}) < \infty$; $\lambda_{\min}(\mathbf{A})$ and $\lambda_{\max}(\mathbf{A})$ represent the smallest and the largest eigenvalue of a matrix $\mathbf{A}$, respectively.

(H.5) Suppose that $\left\| [\zeta(\boldsymbol{x}) - y^s(\boldsymbol{x}, \boldsymbol{\theta})]^6 \right\|_{L_\infty(\boldsymbol{\Omega} \times \boldsymbol{\Theta})} < \infty$.

(H.6) Define $\boldsymbol{\Theta}_0 \subset \boldsymbol{\Theta}$ as a neighborhood of $\boldsymbol{\theta}^*$. Assume there are

    (i) $y^s(\boldsymbol{x}, \boldsymbol{\theta})$ is three times continuously differentiable with respect to $\boldsymbol{\theta}$ in $\boldsymbol{\Theta}_0$;

    (ii) $\frac{\partial y^s(\boldsymbol{x}, \boldsymbol{\theta})}{\partial \theta_{j_1}}$ and $\frac{\partial^2 y^s(\boldsymbol{x}, \boldsymbol{\theta})}{\partial \theta_{j_1} \partial \theta_{j_2}}$ are continuous with respect to $\boldsymbol{x}$ over $\boldsymbol{\Theta}_0$;

    (iii) $\left\| \left[\frac{\partial y^s(\boldsymbol{x}, \boldsymbol{\theta})}{\partial \theta_{j_1}} \right]^9 \right\|_{L_\infty(\boldsymbol{\Omega} \times \boldsymbol{\Theta}_0)} < \infty$;

    (iv) $\left\| \left[\frac{\partial^2 y^s(\boldsymbol{x}, \boldsymbol{\theta})}{\partial \theta_{j_1} \partial \theta_{j_2}} \right]^2 \right\|_{L_\infty(\boldsymbol{\Omega} \times \boldsymbol{\Theta}_0)} < \infty$;

    (v) $\left\| \left[\frac{\partial^3 y^s(\boldsymbol{x}, \boldsymbol{\theta})}{\partial \theta_{j_1} \partial \theta_{j_2} \partial \theta_{j_3}} \right]^2 \right\|_{L_\infty(\boldsymbol{\Omega} \times \boldsymbol{\Theta}_0)} < \infty, \; j_1, j_2, j_3 = 1, \ldots, q.$

(H.7) Assume that $y^s(\boldsymbol{x}_i, \boldsymbol{\theta})$ is $m(\boldsymbol{x}_i)$-Lipschitz continuous. Exactly, $\forall \, \boldsymbol{\theta}_1, \boldsymbol{\theta}_2 \in \boldsymbol{\Theta}$, there

exist $m(\boldsymbol{x}_i)$ such that $|y^s(\boldsymbol{x}_i, \boldsymbol{\theta}_1) - y^s(\boldsymbol{x}_i, \boldsymbol{\theta}_2)| \le m(\boldsymbol{x}_i) \left\| \boldsymbol{\theta}_1 - \boldsymbol{\theta}_2 \right\|_E$.

(H.8) $\max\limits_{i=1,2,\ldots,n} (n\pi_i)^{-1} = O_p(r^{-1})$.

Assumption (H.1) bounds the observation errors. Assumption (H.2) ensures the unique-ness of the OLS estimate. Assumption (H.3) constrains the convergence of the physical observations. Assumption (H.4) ensures positive definiteness of the Hessian matrix. As-sumptions (H.5) – (H.7) are constraints on the smoothness of the computer models. As-sumption (H.8) constrains the weights in (3.1). It is mainly to avoid estimating equations being dominated by data points with extremely small sampling probability. It is common in classical sampling techniques (Breidt and Opsomer, 2000). It can be seen that, relative to the conditions required for the convergence property of the OLS calibration (Wong et al., 2017), only the constraint on the sampling probabilities is added here.

Theorem 1. *If Assumptions (H.1) – (H.8) hold, then as $n \to \infty$ and $r \to \infty$, there is,* $\| \tilde{\boldsymbol{\theta}} - \boldsymbol{\theta}^* \|_E = o_p(r^{-1/2})$ *and*

$$\tilde{\boldsymbol{\theta}} - \boldsymbol{\theta}^* \to N(\boldsymbol{0}, \tilde{\boldsymbol{\Sigma}}^*) \tag{3.4}$$

in distribution. Here, $\tilde{\Sigma}^* = \Sigma + E_{\mathcal{D}_n}(\tilde{\Sigma})$, *where* Σ *is the asymptotic variance-covariance matrix of* $\hat{\boldsymbol{\theta}}$, *which is defined in (2.5) and* $\tilde{\Sigma} = \tilde{\mathbf{J}}^{-1} \tilde{\mathbf{V}} \tilde{\mathbf{J}}^{-1}$ *is the asymptotic variance-covariance matrix of* $\tilde{\boldsymbol{\theta}}$ *conditional on* $\mathcal{D}_n$, *with*

$$\tilde{\mathbf{J}} = \frac{1}{n} \sum_{i=1}^{n} \frac{\partial^2 [y_i^p - \hat{y}^s(\boldsymbol{x}_i, \hat{\boldsymbol{\theta}})]^2}{\partial \boldsymbol{\theta} \partial \boldsymbol{\theta}^T}, \tag{3.5}$$

and

$$\tilde{\mathbf{V}} = \frac{4}{n^2} \sum_{i=1}^{n} \frac{1 - \pi_i}{\pi_i} [y_i^p - \hat{y}^s(\boldsymbol{x}_i, \hat{\boldsymbol{\theta}})]^2 \frac{\partial \hat{y}^s(\boldsymbol{x}_i, \hat{\boldsymbol{\theta}})}{\partial \boldsymbol{\theta}^T} \frac{\partial \hat{y}^s(\boldsymbol{x}_i, \hat{\boldsymbol{\theta}})}{\partial \boldsymbol{\theta}}. \tag{3.6}$$

Indeed, in the cases that the physical observation points do not satisfy the moment conditions in Assumption (H.3), even though $\tilde{\boldsymbol{\theta}}$ does not converge to the true value, $\tilde{\boldsymbol{\theta}}$ can approximate the full data estimate $\hat{\boldsymbol{\theta}}$ efficiently.

Lemma 3.1. *If Assumptions (H.1) – (H.2) and Assumptions (H.4) – (H.8) hold, then as* $n \to \infty$ *and* $r \to \infty$, *there is, conditional on* $\mathcal{D}_n$ *in probability,*

$$\tilde{\Sigma}^{-\frac{1}{2}} (\tilde{\boldsymbol{\theta}} - \hat{\boldsymbol{\theta}}) \to N(\mathbf{0}, \mathbf{I}_q) \tag{3.7}$$

in distribution. Here, $\mathbf{I}_q$ *is the identity matrix of size* q.

From Theorem 1, we know that the uncertainty of $\tilde{\boldsymbol{\theta}}$ can be divided into two parts. First is the uncertainty of $\hat{\boldsymbol{\theta}}$, which arises mainly from the physical observations and the misspecification of the true process $\zeta(\cdot)$. The other one is the uncertainty of $\tilde{\boldsymbol{\theta}}$ given $\mathcal{D}_n$, which is from the subsampling. Moreover, since $\|\hat{\boldsymbol{\theta}} - \boldsymbol{\theta}^*\|_E = O_p(n^{-1/2})$ and $\|\tilde{\boldsymbol{\theta}} - \hat{\boldsymbol{\theta}}\|_E = O_p(r^{-1/2})$, by assuming $r \ll n$, we have that the uncertainty of $\tilde{\boldsymbol{\theta}}$ is mainly captured by the second part. Hence, we focus the the uncertainty arising from the subsampling and improve the accuracy of $\tilde{\boldsymbol{\theta}}$ by choosing $\{\pi_i\}_{i=1}^{n}$ that makes some functional of $\tilde{\mathbf{V}}$ smaller.

3.3 Optimal Poisson Subsampling

As MSE is a commonly used criterion for evaluating the performance of a parameter estimator, we query the optimal subsampling probabilities by minimizing the asymptotic mean square error (AMSE) of $\tilde{\boldsymbol{\theta}}$ given $\mathcal{D}_n$. We abbreviate the criterion as mV-optimal. It corresponds to the A-optimality criterion (Pukelsheim, 2006) in the theory of optimal experimental design and is equivalent to minimizing the trace of $\tilde{\boldsymbol{\Sigma}}$ in Theorem 1. The following theorem gives the result.

Theorem 2. *In Algorithm 1, the subsampling strategy is mV-optimal if the subsampling probabilities are chosen as follows:*

$$\pi_i^{mV} = r\frac{h_i^{mV} \wedge M}{\sum_{j=1}^n (h_j^{mV} \wedge M)}, \ i = 1, \ldots, n, \tag{3.8}$$

where

$$h_i^{mV} = \left|y_i^p - \hat{y}^s(\boldsymbol{x}_i, \hat{\boldsymbol{\theta}})\right| \left[\frac{\partial \hat{y}^s(\boldsymbol{x}_i, \hat{\boldsymbol{\theta}})}{\partial \boldsymbol{\theta}} \tilde{\mathbf{J}}^{-2} \frac{\partial \hat{y}^s(\boldsymbol{x}_i, \hat{\boldsymbol{\theta}})}{\partial \boldsymbol{\theta}^T}\right]^{\frac{1}{2}}. \tag{3.9}$$

Let $h_{(1)}^{mV} \leq h_{(2)}^{mV} \leq \ldots \leq h_{(n)}^{mV}$ be the order statistics of $\{h_i^{mV}\}_{i=1}^n$. For convenience, denote $h_{(n+1)}^{mV} = \infty$ and assume that $h_{(n-r)}^{mV} > 0$, then $M = \frac{1}{r-k} \sum_{i=1}^{n-k} h_{(i)}^{mV}$ and $k = \min\{s \,|\, 0 \leq s \leq r, (r-s)h_{(n-s)}^{mV} < \sum_{i=1}^{n-s} h_{(i)}^{mV}\}$.

As shown in Theorem 2, the optimal subsampling probabilities $\{\pi_i^{mV}\}_{i=1}^n$ depend on data through both covariates and responses. The inclusion of data points with lager values of $\left|y_i^p - \hat{y}^s(\boldsymbol{x}_i, \hat{\boldsymbol{\theta}})\right|$ and $\left[\frac{\partial \hat{y}^s(\boldsymbol{x}_i, \hat{\boldsymbol{\theta}})}{\partial \boldsymbol{\theta}} \tilde{\mathbf{J}}^{-2} \frac{\partial \hat{y}^s(\boldsymbol{x}_i, \hat{\boldsymbol{\theta}})}{\partial \boldsymbol{\theta}^T}\right]$ will improve the robustness of the subsample estimator. A larger value of $\left|y_i^p - \hat{y}^s(\boldsymbol{x}_i, \hat{\boldsymbol{\theta}})\right|$ means that the calibrated computer output differs more from the physical observation at $\boldsymbol{x}_i$. Since $\|\hat{\boldsymbol{\theta}} - \boldsymbol{\theta}^*\|_E = o_p(n^{-1/2})$, the distance between the physical observation and the calibrated computer output is dominated by the observation error and the model discrepancy $\zeta(\cdot) - y^s(\cdot, \boldsymbol{\theta}^*)$. The matrix $\frac{1}{n} \sum_{i=1}^n \left[\frac{\partial \hat{y}^s(\boldsymbol{x}, \hat{\boldsymbol{\theta}})}{\partial \boldsymbol{\theta}^T} \frac{\partial \hat{y}^s(\boldsymbol{x}_i, \hat{\boldsymbol{\theta}})}{\partial \boldsymbol{\theta}}\right]$ is

the fisher information matrix of $\hat{\boldsymbol{\theta}}$ in the cases that the computer model $y^s(\cdot, \boldsymbol{\theta}^*)$ is perfect, i.e., $\zeta(\cdot) = y^s(\cdot, \boldsymbol{\theta}^*)$. Therefore, intuitively, larger $\left[\frac{\partial \hat{y}^s(\boldsymbol{x}_i, \hat{\boldsymbol{\theta}})}{\partial \boldsymbol{\theta}} \tilde{\mathbf{J}}^{-2} \frac{\partial \hat{y}^s(\boldsymbol{x}_i, \hat{\boldsymbol{\theta}})}{\partial \boldsymbol{\theta}^T}\right]$ indicates that $\boldsymbol{x}_i$ carries more information about the calibration parameters.

Evaluating the optimal subsampling probabilities requires the calculation of $\tilde{\mathbf{J}}$, whose computational complexity is $O(q^2 n)$. By adding the computational time of predicting the computer outputs and calculating the first derivative of the computer model at $\{(\boldsymbol{x}_i, \hat{\boldsymbol{\theta}})\}_{i=1}^n$, the computational complexity of evaluating $\{h_1^{mV}, \ldots, h_n^{mV}\}$ is $O(q^2 n + q^3 n + m^3 + mn)$ for given $\hat{\boldsymbol{\theta}}$. To save the computational time, following from Wang et al. (2018), the optimal probabilities can be evaluated by minimizing $\text{tr}(\tilde{\mathbf{V}})$. We abbreviate this criterion as mVc-optimal. It is called L-optimality in optimal experimental design (Pukelsheim, 2006). The result is presented in the following theorem.

Theorem 3. *In Algorithm 1, the subsampling strategy is mVc-optimal if the subsampling probabilities are chosen as follows:*

$$\pi_i^{mVc} = r \frac{h_i^{mVc} \wedge M}{\sum_{j=1}^n (h_j^{mVc} \wedge M)}, \ i = 1, \ldots, n, \tag{3.10}$$

where

$$h_i^{mVc} = \left| y_i^p - \hat{y}^s(\boldsymbol{x}_i, \hat{\boldsymbol{\theta}}) \right| \left[\frac{\partial \hat{y}^s(\boldsymbol{x}_i, \hat{\boldsymbol{\theta}})}{\partial \boldsymbol{\theta}} \frac{\partial \hat{y}^s(\boldsymbol{x}_i, \hat{\boldsymbol{\theta}})}{\partial \boldsymbol{\theta}^T}\right]^{\frac{1}{2}}. \tag{3.11}$$

Let $h_{(1)}^{mVc} \leq h_{(2)}^{mVc} \leq \ldots \leq h_{(n)}^{mVc}$ *be the order statistics of* $\{h_i^{mVc}\}_{i=1}^n$. *For convenience, denote* $h_{(n+1)}^{mVc} = \infty$ *and assume that* $h_{(n-r)}^{mVc} > 0$, *then* $M = \frac{1}{r-k} \sum_{i=1}^{n-k} h_{(i)}^{mVc}$ *and* $k = \min\{s \mid 0 \leq s \leq r, (r-s) h_{(n-s)}^{mVc} < \sum_{i=1}^{n-s} h_{(i)}^{mVc}\}$.

It can be seen that the alternative optimization criterion does reduces the computing time since there is no need to calculate $\tilde{\mathbf{J}}$ and $\tilde{\mathbf{J}}^{-1}$. The computational complexity of evaluating $\{h_1^{mVc}, \ldots, h_n^{mVc}\}$ is reduced to $O(q^2 n + m^3 + mn)$ for given $\hat{\boldsymbol{\theta}}$.

For ease of writing, we use a unified notation π_i^{opt} to denote π_i^{mV} and π_i^{mVc} in Theorem

[2](#) and Theorem [3](#), that is,

$$\pi_i^{opt} = r\frac{h_i^{opt} \wedge M}{\sum_{j=1}^n (h_j^{opt} \wedge M)} = r\frac{h_i^{opt} \wedge M}{n\Psi}, \ i = 1, \dots, n, \tag{3.12}$$

where $M = \frac{1}{r-k}\sum_{i=1}^{n-k} h_{(i)}^{opt}$, $\Psi = \frac{1}{n}\sum_{j=1}^n (h_j^{opt} \wedge M)$, and h_i^{opt} is used to refer to h_i^{mV} or h_i^{mVc}.

Lemma 3.2. *If the subsampling probabilities in Algorithm [1](#) are chosen as π_i^{opt}, then the AMSE of $\tilde{\boldsymbol{\theta}}$ given $\mathcal{D}_n$ can be represented by*

$$\frac{4}{n^2(r-k)}\left[\sum_{i=1}^{n-k} h_{(i)}^{opt}\right]\sum_{i=1}^{n-k}\left\{\frac{[h_{(i)}^{mV}]^2}{h_{(i)}^{opt}}\right\} - \frac{4}{n^2}\sum_{i=1}^{n-k}\left[h_{(i)}^{mV}\right]^2. \tag{3.13}$$

Specifically, if the optimal subsampling probabilities is chosen as π_i^{mV}, then the AMSE of $\tilde{\boldsymbol{\theta}}$ given $\mathcal{D}_n$ is the minimum, which can be represented by

$$\frac{4}{n^2(r-k)}\left[\sum_{i=1}^{n-k} h_{(i)}^{mV}\right]^2 - \frac{4}{n^2}\sum_{i=1}^{n-k}\left[h_{(i)}^{mV}\right]^2. \tag{3.14}$$

As reported in Yu et al. (2022), k tends to be zero as r/n becomes smaller. By setting $k = 0$, we have that the minimum AMSE of $\tilde{\boldsymbol{\theta}}$ depends on the mean and dispersion of $h_1^{mV}, \dots, h_n^{mV}$. The full data with small and dispersed $\{h_i^{mV}\}_{i=1}^n$ will deduce small minimum AMSE, if the subsamples are obtained according to the mV criterion. Since $\mathcal{D}_n$ is fixed before subsampling, this part is not discussed further. Besides the full data, it can be seen that, the minimum AMSE depends on the subsamples size. To obtain more accurate parameter estimators, a larger amount of subsamples is preferred.

4 Implementation of the IPWLS Calibration

The optimal probabilities in (3.8) and (3.10) depend on $\hat{\boldsymbol{\theta}}$, $\tilde{\mathbf{J}}$, M and Ψ, which are calculated by using the full data. Thus, an exact IPWLS estimator for the calibration parameters by using Algorithm [1](#) can't be obtained directly. We propose a two-step algorithm to approximate the IPWLS estimator in this section.

4.1 Two-step Algorithm

To practically implement the optimal probabilities, we need to replace $\hat{\boldsymbol{\theta}}$ and $\tilde{\mathbf{J}}$ with their respective pilot estimator $\tilde{\boldsymbol{\theta}}_0$ and $\tilde{\mathbf{J}}_0$, which can be obtained by a uniform subsample of r_0 with $r_0 < n$. Denote S_{r_0} as the set of the pilot subsamples and $|S_{r_0}|$ is the size of S_{r_0}. The pilot estimator $\tilde{\boldsymbol{\theta}}_0$ and $\tilde{\mathbf{J}}_0$ can be expressed respectively as

$$\tilde{\boldsymbol{\theta}}_0 = \arg\min_{\boldsymbol{\theta} \in \boldsymbol{\Theta}} \frac{1}{|S_{r_0}|} \sum_{S_{r_0}} [y_i^p - \hat{y}^s(\boldsymbol{x}_i, \boldsymbol{\theta})]^2, \tag{4.1}$$

and

$$\tilde{\mathbf{J}}_0 = \frac{1}{|S_{r_0}|} \sum_{S_{r_0}} \frac{\partial^2 [y_i^p - \hat{y}^s(\boldsymbol{x}_i, \tilde{\boldsymbol{\theta}}_0)]^2}{\partial \boldsymbol{\theta} \partial \boldsymbol{\theta}^T}. \tag{4.2}$$

Furthermore, to determine the subsampling probability of each data point separately, we use the pilot sample to approximate M and Ψ. Following Yu et al. (2022), choosing $M = \infty$ will not have a significant impact on the optimal subsampling probabilities as long as r/n is small. Thus, we set $M = \infty$ and

$$\Psi_0 = \frac{1}{|S_{r_0}|} \sum_{S_{r_0}} \left| y_i^p - \hat{y}^s(\boldsymbol{x}_i, \tilde{\boldsymbol{\theta}}_0) \right| \psi_0(\boldsymbol{x}_i), \tag{4.3}$$

where $\psi_0(\boldsymbol{x}_i) = \left[\frac{\partial \hat{y}^s(\boldsymbol{x}_i, \tilde{\boldsymbol{\theta}}_0)}{\partial \boldsymbol{\theta}} \tilde{\mathbf{J}}_0^{-2} \frac{\partial \hat{y}^s(\boldsymbol{x}_i, \tilde{\boldsymbol{\theta}}_0)}{\partial \boldsymbol{\theta}^T} \right]^{1/2}$ for the mV criterion, and $\psi_0(\boldsymbol{x}_i) = \left[\frac{\partial \hat{y}^s(\boldsymbol{x}_i, \tilde{\boldsymbol{\theta}}_0)}{\partial \boldsymbol{\theta}} \frac{\partial \hat{y}^s(\boldsymbol{x}_i, \tilde{\boldsymbol{\theta}}_0)}{\partial \boldsymbol{\theta}^T} \right]^{1/2}$ for the mVc criterion.

Denote $\breve{\pi}_i^{opt}$ be the approximated subsampling probabilities with $\hat{\boldsymbol{\theta}}$, $\tilde{\mathbf{J}}$, M Ψ, and r in (3.12) replaced by their respective pilot estimate, i.e.

$$\breve{\pi}_i^{opt} = r \frac{\left| y_i^p - \hat{y}^s(\boldsymbol{x}_i, \tilde{\boldsymbol{\theta}}_0) \right| \psi_0(\boldsymbol{x}_i)}{n \Psi_0}, \quad i = 1, \dots, n. \tag{4.4}$$

The estimator with $\breve{\pi}_i^{opt}$ inserted in (3.1) may be sensitive to the data points with $y_i^p - \hat{y}^s(x_i, \tilde{\boldsymbol{\theta}}_0) \approx 0$ if they are included in the subsamples. A small nugget can be added to $\breve{\pi}_i^{opt}$ to make the estimator more robust. Consider an extreme case, if $y_i^p - \hat{y}^s(x_i, \tilde{\boldsymbol{\theta}}_0)$ is zero

16

for all $\boldsymbol{x}_i$, then $\tilde{\boldsymbol{\theta}}_0$ is accurate. In this case, the optimal subsampling probabilities should be the uniform subsampling probabilities that used to generate the pilot subsamples. As a result, we use the uniform subsampling probabilities as the nugget. Precisely, we use the following subsampling probabilities $\breve{\pi}_i^w$, which is a convex combination of $\breve{\pi}_i^{opt}$ in (4.4) and the uniform subsampling probabilities,

$$\breve{\pi}_i^w = (1-\rho)r\frac{\left|y_i^p - \hat{y}^s(\boldsymbol{x}_i, \tilde{\boldsymbol{\theta}}_0)\right|\psi_0(\boldsymbol{x}_i)}{n\Psi_0} + \rho r\frac{1}{n}, \; i = 1, \ldots, n, \tag{4.5}$$

where $\rho \in (0, 1)$. This weighted adjustment is also used in Ma et al. (2014) and Yu et al. (2022). When ρ is larger, the corresponding estimator will be more robust since $l^*(\boldsymbol{\theta})$ in (3.1) will not be inflated by data points with extremely small values of $\breve{\pi}_i^{opt}$.

Considering some $\breve{\pi}_i^w$ may be larger than one due to approximated Ψ and taking $M = \infty$, we need to use the inverse of $\breve{\pi}_i^w \wedge 1$'s as weights. Since $\breve{\pi}_i^w \wedge 1$ depends only on $\boldsymbol{x}_i$, y_i^p, $\hat{y}^s(\boldsymbol{x}_i, \tilde{\boldsymbol{\theta}}_0)$ and $\frac{\partial \hat{y}^s(\boldsymbol{x}_i, \tilde{\boldsymbol{\theta}}_0)}{\partial \boldsymbol{\theta}}$, each $\breve{\pi}_i^w$ can be calculated independently. That is, there is no need to calculate all $\breve{\pi}_i^w, i = 1, \ldots, n$ at once. Thus, there is not need to load the full data into memory and this is very computationally beneficial in terms of memory usage. The practical implementation above is summarized in Algorithm 2.

The optimal sampling probability at each physical sample are required in Algorithm 2. That is, the prediction and the derivative of the computer outputs at $\{\boldsymbol{x}_i, \tilde{\boldsymbol{\theta}}_0\}_{i=1}^n$ is required once in this Algorithm. It leads that the the computational complexity of evaluating $\breve{\boldsymbol{\theta}}$ becomes $O(nm + nq^3 + w_r(r_0 + r)q^2 + w_r(r_0 + r)m + m^3)$ for the mV criterion and $O(nm + nq^2 + w_r(r_0 + r)q^2 + w_r(r_0 + r)m + m^3)$ for the mVc criterion.

4.2 Asymptotic Properties

For the estimator obtained from Algorithm 2, now we establish its consistency and asymptotic normality.

Algorithm 2: Two-step Algorithm

Step 1: Run Algorithm 1 with subsample size r_0 and uniform subsampling

probability $\boldsymbol{\pi}^{unif} = \{\frac{r_0}{n}\}_{i=1}^{n}$ to get a subsample set S_{r_0}. Use S_{r_0} to obtain the pilot

estimates $\tilde{\boldsymbol{\theta}}_0$ from (4.1), $\tilde{\mathbf{J}}_0$ from (4.2), and Ψ_0 from (4.3).

Step 2: Set $S_0 = S_{r_0}$ and $\pi_i = \breve{\pi}_i^w$, where $\breve{\pi}_i^w$ is defined in (4.5). Run Algorithm 1

to collect the subsample set $S_r = \{(\boldsymbol{x}_i^*, y^p(\boldsymbol{x}_i^*), \breve{\pi}_i^w \wedge 1)\}_{i=1}^{r}$ and obtain $\breve{\boldsymbol{\theta}}$ based on

the subsamples by solving the following minimization problem

$$\breve{\boldsymbol{\theta}} := \arg\min_{\boldsymbol{\theta} \in \Theta} l_{\tilde{\boldsymbol{\theta}}_0}^*(\boldsymbol{\theta}), \tag{4.6}$$

where

$$l_{\tilde{\boldsymbol{\theta}}_0}^*(\boldsymbol{\theta}) = \frac{1}{n} \sum_{i=1}^{r} \frac{1}{\breve{\pi}_i^w \wedge 1} \left[y^p(\boldsymbol{x}_i^*) - \hat{y}^s(\boldsymbol{x}_i^*, \boldsymbol{\theta}) \right]^2. \tag{4.7}$$

Theorem 4. *If Assumptions (H.1) – (H.8) hold and $r_0 r^{-\frac{1}{2}} \to 0$, then as $r \to \infty$ and*

$n \to \infty$, $\breve{\boldsymbol{\theta}}$ is consistent to $\boldsymbol{\theta}^*$ in probability.

In fact, as long as the pilot estimator $\tilde{\boldsymbol{\theta}}_0$ exists, Algorithm 2 will produce a consistent

estimator. We don't have to limit $r_0 \to \infty$ in Theorem 4. Of course, if $r_0 \to \infty$, we can

get from Theorem 1 that $\tilde{\boldsymbol{\theta}}_0$ exists with probability approaching one.

Theorem 5. *If Assumptions (H.1) – (H.8) hold and $r_0 r^{-\frac{1}{2}} \to 0$, then as $r_0 \to \infty$, $r \to \infty$*

and $n \to \infty$, there is $\|\breve{\boldsymbol{\theta}} - \boldsymbol{\theta}^*\|_E = o_p(r^{-1/2})$ and

$$\breve{\boldsymbol{\theta}} - \boldsymbol{\theta}^* \to N(\mathbf{0}, \breve{\boldsymbol{\Sigma}}^*) \tag{4.8}$$

in distribution. Here, $\breve{\boldsymbol{\Sigma}}^* = \mathrm{E}_{\mathcal{D}_n}(\breve{\boldsymbol{\Sigma}}) + \boldsymbol{\Sigma}$, where $\breve{\boldsymbol{\Sigma}} = \tilde{\mathbf{J}}^{-1} \tilde{\mathbf{V}}^w \tilde{\mathbf{J}}^{-1}$, and

$$\tilde{\mathbf{V}}^w = \frac{4}{n^2} \sum_{i=1}^{n} \frac{1 - \pi_i^w \wedge 1}{\pi_i^w \wedge 1} [y_i^p - \hat{y}^s(\boldsymbol{x}_i, \hat{\boldsymbol{\theta}})]^2 \frac{\partial \hat{y}^s(\boldsymbol{x}_i, \hat{\boldsymbol{\theta}})}{\partial \boldsymbol{\theta}^T} \frac{\partial \hat{y}^s(\boldsymbol{x}_i, \hat{\boldsymbol{\theta}})}{\partial \boldsymbol{\theta}},$$

with

$$\pi_i^w = (1 - \rho)r\frac{h_i^{mV}}{\sum_{j=1}^n h_j^{mV}} + \rho r\frac{1}{n},$$

for the mV criterion and

$$\pi_i^w = (1 - \rho)r\frac{h_i^{mVc}}{\sum_{j=1}^n h_j^{mVc}} + \rho r\frac{1}{n},$$

for the mVc criterion.

In Theorem 5, we require $r_0 \to \infty$ to get a consistent pilot estimate which is used to identify the more informative data points in the second step. On the other hand, r_0 should be much smaller than r so that the more informative second step subsample dominates the weighted loss function.

Lemma 4.1. *If Assumptions (H.1) – (H.2) and Assumptions (H.4) – (H.8) hold, and $r_0 r^{-\frac{1}{2}} \to 0$, then as $r_0 \to \infty$, $r \to \infty$ and $n \to \infty$, there is, conditional on $\mathcal{D}_n$ in probability,*

$$\breve{\boldsymbol{\Sigma}}^{-\frac{1}{2}}(\breve{\boldsymbol{\theta}} - \hat{\boldsymbol{\theta}}) \to N(\mathbf{0}, \mathbf{I}_q) \tag{4.9}$$

in distribution.

Lemma 4.2. *Assume that $r \ll n$. The AMSE of $\breve{\boldsymbol{\theta}}$ given $\mathcal{D}_n$ can be represented by*

$$\frac{4}{nr}\left[\frac{1}{n}\sum_{j=1}^n h_j^{mV}\right]\left[\sum_{i=1}^n \frac{(h_i^{mV})^2}{(1-\rho)h_i^{mV} + \rho\frac{1}{n}\sum_{j=1}^n h_j^{mV}}\right] - \frac{4}{n^2}\sum_{i=1}^n (h_i^{mV})^2 \tag{4.10}$$

for the mV criterion and

$$\frac{4}{nr}\left[\frac{1}{n}\sum_{j=1}^n h_j^{mVc}\right]\left[\sum_{i=1}^n \frac{(h_i^{mV})^2}{(1-\rho)h_i^{mVc} + \rho\frac{1}{n}\sum_{j=1}^n h_j^{mVc}}\right] - \frac{4}{n^2}\sum_{i=1}^n (h_i^{mV})^2 \tag{4.11}$$

for the mVc criterion.

By some easy calculations, if $\rho = 1$, the AMSE of $\breve{\boldsymbol{\theta}}$ given $\mathcal{D}_n$ is $\frac{4}{r}\left[\frac{1}{n}\sum_{i=1}^n (h_i^{mV})^2\right] - \frac{4}{n^2}\sum_{i=1}^n (h_i^{mV})^2$. If $\rho = 0$, the AMSE of $\breve{\boldsymbol{\theta}}$ given $\mathcal{D}_n$ is $\frac{4}{r}\left[\frac{1}{n}\sum_{i=1}^n h_i^{mV}\right]^2 - \frac{4}{n^2}\sum_{i=1}^n (h_i^{mV})^2$ for

the mV criterion. Since $\left[\frac{1}{n}\sum_{i=1}^n (h_i^{mV})^2\right] \geq \left[\frac{1}{n}\sum_{i=1}^n h_i^{mV}\right]^2$, together with Theorem 2, we have that, by carefully choosing ρ, the two-step algorithm is asymptotically more efficient than the uniform subsampling. That is, $\tilde{\boldsymbol{\theta}}_0$ is also asymptotically normal from Theorem 1, but the trace of its asymptotic variance is larger than that for the two-step IPWLS estimator with the same subsample size.

4.3 Uncertainty Quantification of the IPWLS Estimator

Estimating the variance of the proposed estimator is crucial for statistical inferences such as hypothesis testing and confidence interval construction. As mentioned before, the uncertainty of the $\hat{\boldsymbol{\theta}}$ can be ignored when $r \ll n$. We use the variance of $\breve{\boldsymbol{\theta}}$ conditional on $\mathcal{D}_n$ to approximate its unconditional variance. When physical observations are limited, the bootstrap approach and Markov chain Monte Carlo (MCMC) method are widely used to estimate the variance of a frequency estimator (Wong et al., 2017) and a Bayesian estimator (Kennedy and O'Hagan, 2001), respectively. Unfortunately, the bootstrap method and MCMC method lose their advantages when the physical observations are massive due to their time-consuming computation. Thus, an explicit expression for the conditional variance of $\breve{\boldsymbol{\theta}}$ is preferred to simplify the computation.

Note that, although we require $r \ll n$, in fact, the choice of r can be relatively large. Thus we use the asymptotic variance-covariance matrix $\breve{\boldsymbol{\Sigma}}$ in Theorem 5 to get the estimated version. This method is widely used in the uncertainty quantification for parameter estimation with large samples (Wang et al., 2018). This approach, however, requires calculations on the full data. Following Wang et al. (2018), variance-covariance matrix of $\breve{\boldsymbol{\theta}}$ given $\mathcal{D}_n$ can be estimated by using the subsamples S_r. Specifically, let $\Psi_r = \frac{1}{r}\sum_{i=1}^r \left| y^p(\boldsymbol{x}_i^*) - \hat{y}^s(\boldsymbol{x}_i^*, \tilde{\boldsymbol{\theta}}_0) \right| \psi_r(\boldsymbol{x}_i^*)$ with $\psi_r(\boldsymbol{x}_i^*) = \left[\frac{\partial \hat{y}^s(\boldsymbol{x}_i^*, \tilde{\boldsymbol{\theta}}_0)}{\partial \boldsymbol{\theta}} \tilde{\mathbf{J}}_0^{-2} \frac{\partial \hat{y}^s(\boldsymbol{x}_i^*, \tilde{\boldsymbol{\theta}}_0)}{\partial \boldsymbol{\theta}^T} \right]^{1/2}$ for the

mV criterion, and $\psi_r(\boldsymbol{x}_i) = \left[\frac{\partial \hat{y}^s(\boldsymbol{x}_i^*, \tilde{\boldsymbol{\theta}}_0)}{\partial \boldsymbol{\theta}} \frac{\partial \hat{y}^s(\boldsymbol{x}_i^*, \tilde{\boldsymbol{\theta}}_0)}{\partial \boldsymbol{\theta}^T}\right]^{1/2}$ for the mVc criterion. We propose that $\breve{\boldsymbol{\Sigma}}$ can be approximated by

$$\breve{\boldsymbol{\Sigma}}_r = \breve{\mathbf{J}}_r^{-1} \breve{\mathbf{V}}_r^w \breve{\mathbf{J}}_r^{-1}, \tag{4.12}$$

with

$$\breve{\mathbf{J}}_r = \frac{1}{n} \sum_{S_r} \frac{1}{\breve{\pi}_i^r \wedge 1} \frac{\partial^2 [y^p(\boldsymbol{x}_i^*) - \hat{y}^s(\boldsymbol{x}_i^*, \breve{\boldsymbol{\theta}})]^2}{\partial \boldsymbol{\theta} \partial \boldsymbol{\theta}^T}, \tag{4.13}$$

and

$$\breve{\mathbf{V}}_r^w = \frac{4}{n^2} \sum_{S_r} \frac{1 - \breve{\pi}_i^r \wedge 1}{(\breve{\pi}_i^r \wedge 1)^2} [y^p(\boldsymbol{x}_i^*) - \hat{y}^s(\boldsymbol{x}_i^*, \breve{\boldsymbol{\theta}})]^2 \frac{\partial \hat{y}^s(\boldsymbol{x}_i^*, \breve{\boldsymbol{\theta}})}{\partial \boldsymbol{\theta}^T} \frac{\partial \hat{y}^s(\boldsymbol{x}_i^*, \breve{\boldsymbol{\theta}})}{\partial \boldsymbol{\theta}}, \tag{4.14}$$

where

$$\breve{\pi}_i^r = (1 - \rho) r \frac{\left| y^p(\boldsymbol{x}_i^*) - \hat{y}^s(\boldsymbol{x}_i^*, \tilde{\boldsymbol{\theta}}_0) \right| \psi_r(\boldsymbol{x}_i)}{n \Psi_r} + \rho r \frac{1}{n}. \tag{4.15}$$

The above formula involves only the selected subsamples to estimate the conditional variance-covariance matrix. Based on the method of moments, if $\breve{\boldsymbol{\theta}}$ is replaced by $\hat{\boldsymbol{\theta}}$, $\breve{\mathbf{J}}_r$ and $\breve{\mathbf{V}}_r^w$ are unbiased estimators of $\tilde{\mathbf{J}}$ and $\tilde{\mathbf{V}}^w$, respectively.

In addition to uncertainty quantification, the variance-covariance matrix $\breve{\boldsymbol{\Sigma}}_r$ helps to determine the subsample size. Specifically, by pre-setting the width of the confidence band for parameter estimation, we can judge whether the current subsamples are sufficient. If the current confidence interval is too wide, the accuracy of parameter estimation can be achieved by adding more samples.

5   Numerical Studies

In this section, we evaluate the performance of the proposed estimator through some simulations. Since the maximin distance design is asymptotically optimum for building $\hat{y}^s$ under a Bayesian setting (Johnson et al., 1990), we adopt the Maximin Latin-hypercube

design (Santner et al., 2018) to conduct the computer experiments. The common choice of m is $m \geq 10(d + q)$, as recommended in Loeppky and Welch (2009). To get a decent $\tilde{\boldsymbol{\theta}}_0$, following Krishna et al. (2021), we set r_0 on $2q + 10d$. To balance the robustness and accuracy of the proposed estimator, following Yu et al. (2022); Wang et al. (2018), we set $\rho = 0.2$. The performance of the optimal subsampling probability is examined by the following criterion:

$$\text{RMSE} = \frac{1}{T} \sum_{t=1}^{T} \sum_{j=1}^{q} \left[\frac{\breve{\theta}_j^{(t)} - \theta_j^*}{\theta_j^*} \right]^2,$$

where $\breve{\boldsymbol{\theta}}^{(t)}$ is the estimator obtained from the t-th subsamples with the optimal subsampling probabilities. We set $T = 100$ throughout this section.

5.1   Simulation Studies

Example 1.   Suppose the computer model is

$$y^s(x, \boldsymbol{\theta}) = 7[\sin(2\pi\theta_1 - \pi)]^2 + 2(2\pi\theta_2 - \pi)^2 \sin(2\pi x - \pi), \tag{5.1}$$

where $x \in [0, 1]$, $\boldsymbol{\theta} \in [0, 0.25] \times [0, 0.5]$. Suppose the true process $\zeta(x) = y^s(x, \boldsymbol{\theta}^*)$, with $\boldsymbol{\theta}^* = [0.2, 0.3]^T$. The total number of samples n is 10000 and suppose the observation errors $e_i \sim N(0, 0.2^2)$.

Now we compare the calculation time and accuracy of the proposed estimator for three different subsampling criteria: uniform subsampling, mV and the mVc subsampling. The first step sample size r_0 is fixed on 14, and r is from $\{100, 200, 300, 400, 600\}$. Since the uniform subsampling probability does not depend on unknown parameters and no pilot subsamples are required, it is implemented with subsample size $r_0 + r$ for fair.

The calculation time for evaluating the estimator with different subsample sizes are shown in Table 1. The calculation time for using the full data is also given for compar-

22

isons. It can be seen that by using the subsamples, the computational time to evaluate

Table 1: Calculation time (seconds) v.s. different subsample sizes

Criterion	$r = 100$	$r = 200$	$r = 300$	$r = 400$	$r = 600$	$r = n = 10000$
uniform	0.051	0.076	0.094	0.117	0.126	0.952
mV	0.205	0.227	0.250	0.270	0.285	1.379
mVc	0.188	0.195	0.204	0.249	0.257	1.294

the estimator is greatly saved. The estimator based on the uniform subsampling method requires the least computing time since it does not need to calculate the subsampling probabilities. Because the optimal subsampling probabilities for the mV subsampling criterion require the calculation of $\tilde{\mathbf{J}}$, evaluating the estimator based on the mV subsampling criterion is more time-consuming than that based on the mVc criterion.

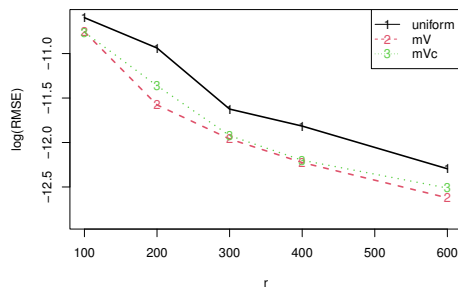Figure 1 shows the comparison of the accuracy for the proposed estimator. The esti-

Figure 1: Accuracy of the proposed estimator for different subsample sizes r and a fixed $r_0 = 14$ based on mV (red), mVc (green) and uniform (black) subsampling methods.

mators by using the mV and mVc subsampling methods achieve smaller RMSEs. These results agree with the theoretical results in Section 3.

The results of the relationship between subsamples and subsampling probabilities are presented in Figure 2. Combined with Figure 1, it states that the subsampling probabilities
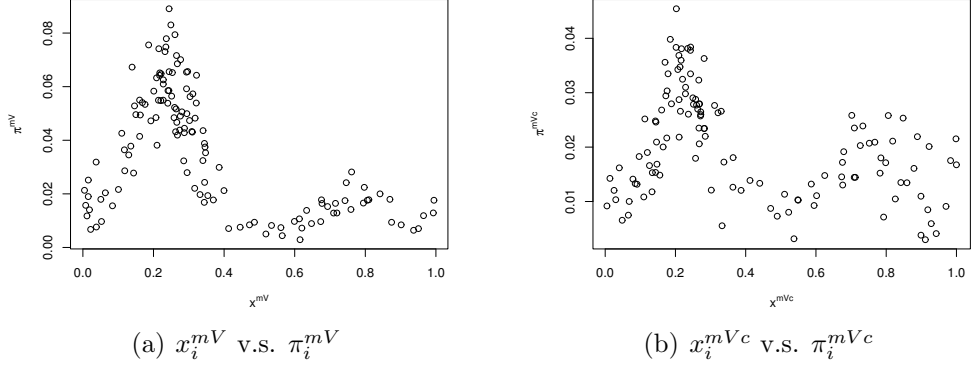
(a) x_i^{mV} v.s. π_i^{mV} (b) x_i^{mVc} v.s. π_i^{mVc}

Figure 2: The relationship between subsamples and subsampling probabilities based on mV and mVc methods with $r = 100$.

based on the mV and mVc criteria make full use of the information contained in the subsamples, which is not available in uniform subsampling, and this is why the two criteria have smaller RMSEs. In Figure 2, where π_i^{mV} and π_i^{mVc} are larger, the corresponding $\frac{\partial \hat{y}^s(\boldsymbol{x}_i^*, \check{\boldsymbol{\theta}})}{\partial \boldsymbol{\theta}}$ is also larger, which is consistent with the results in Theorem 2 and Theorem 3.

To assess the performance of the proposed subsampling method for statistical inference, the standard error given in (4.12) is used to estimate the variance-covariance matrices based on selected subsamples. We take θ_2 as an example and present its coverage rates and lengths of 95% confidence intervals in Table 2. Because the lengths of confidence intervals

Table 2: Average lengths and coverage rates of 95% confidence intervals for θ_2.

Criterion	uniform		mV		mVc	
	length	coverage rate	length	coverage rate	length	coverage rate
$r = 100$	0.0047	0.96	0.0040	0.96	0.0042	0.99
$r = 200$	0.0034	0.96	0.0029	0.98	0.0029	0.94
$r = 300$	0.0027	0.97	0.0023	0.95	0.0023	0.95
$r = 400$	0.0024	0.98	0.0019	0.94	0.0020	0.96
$r = 600$	0.0019	0.99	0.0016	0.93	0.0016	0.96

calculated by the uniform based subsampling method are the longest, its coverage rates at some sample sizes are slightly larger than that of the mV and mVc based subsampling methods. We can also obtain that the subsampling methods based on mV and mVc require fewer subsamples than that based on uniform to achieve considerable statistical inference effect. In general, mV and mVc subsampling methods outperform the uniform subsampling method.

Example 2. Suppose $\zeta(\cdot)$ can be expresses as

$$\zeta(\boldsymbol{x}) = \frac{x_1}{2}\left[\sqrt{1+(x_1+x_3^2)\frac{x_4}{x_1^2}}-1\right]+(x_1+3x_4)\exp[1+\sin(x_3)]$$

and the computer model (Xiong et al., 2013) is

$$y^s(\boldsymbol{x},\boldsymbol{\theta}) = (\theta_1+\frac{\sin(x_1)}{10})\zeta(\boldsymbol{x})+\theta_2(-2x_1+x_2^2+x_3^2)+0.5,$$

where θ_1 and θ_2 are two calibration parameters, with $\boldsymbol{\theta} \in [-5,5]^2$, and $\boldsymbol{x} \in [0,1]^4$. Let $\boldsymbol{X} = \{\boldsymbol{x}_1, \boldsymbol{x}_2, \ldots, \boldsymbol{x}_n\}$ be the set of design points in a MmLHDs, with $n = 10000$; e_i's are mutually independent and follow $N(0, 0.1^2)$. We apply BB algorithm (Varadhan and Gilbert, 2010) to find that the local optimal point $\boldsymbol{\theta}^* = [0.895, 0.267]^T$. To investigate the performance of the proposed method, we select the subsamples with the subsample size equals to 400, 500, 600, 700, and 800, respectively.

The computational time for different subsample sizes under the three subsampling criteria are summarized in Table 3. To assess the performance of Algorithm 2 under three subsampling probabilities, we also evaluate the RMSE for the three different subsampling criteria. Figure 3 compares the accuracy of different estimators. It can be concluded that the estimators obtained by using the mV and mVc subsampling methods outperform that obtained by using the uniform subsampling method. Otherwise, RMSE decreases as r increases, which confirms the theoretical result on the consistency of the subsampling

Table 3: Calculation time (seconds) v.s. different subsample sizes

Criterion	$r = 400$	$r = 500$	$r = 600$	$r = 800$	$r = 900$	$r = n = 10000$
uniform	0.150	0.153	0.168	0.179	0.237	1.517
mV	0.360	0.371	0.429	0.492	0.5338	1.581
mVc	0.316	0.360	0.367	0.458	0.493	1.531
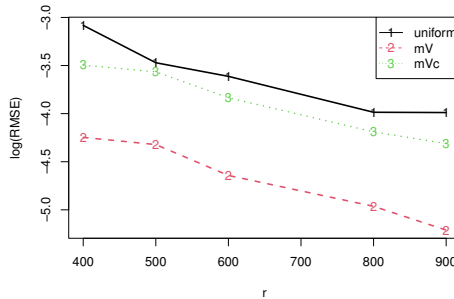
Figure 3: Accuracy of the proposed estimator for different subsample sizes r and a fixed $r_0 = 44$ based on mV (red), mVc (green) and uniform (black) subsampling methods.

methods.

Combining Figure 3 and Figure 4, we can also conclude that the uniform subsampling method does not make full use of the information contained in the subsamples, so it is not as good as the subsampling method based on mV and mVc.

Similarly, we get 95% confidence intervals of parameters based on uniform, mV and mVc subsampling methods by simple calculation. As an example, we take θ_2 as the parameter of interest. The average lengths and coverage rates of confidence intervals are reported in Table 4. It shows that mV and mVc based subsampling methods have similar performances and they both perform better than uniform subsampling method. At some sample points, the coverage rates of uniform based subsampling method is greater than that of mVc based subsampling method because its corresponding confidence interval length is the longest. As
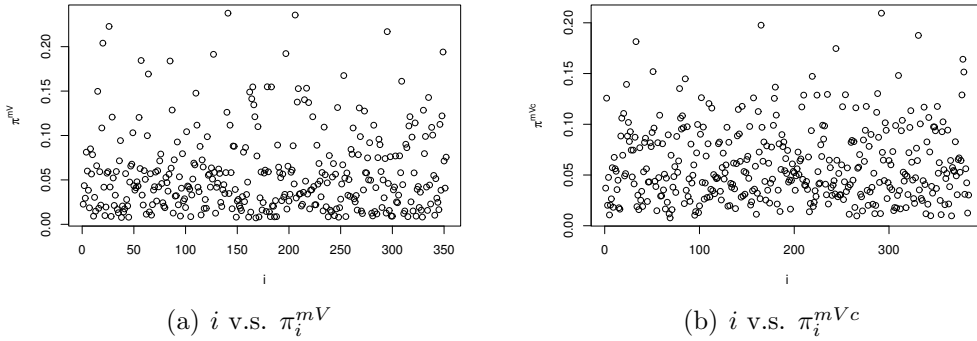
(a) i v.s. π_i^{mV} (b) i v.s. π_i^{mVc}

Figure 4: The distribution of subsampling probabilities based on mV and mVc methods with $r = 400$.

Table 4: Average lengths and coverage rates of 95% confidence intervals for θ_2.

Criterion	uniform		mV		mVc	
	length	coverage rate	length	coverage rate	length	coverage rate
$r = 400$	0.208	0.92	0.135	0.96	0.180	0.93
$r = 500$	0.187	0.97	0.117	0.96	0.166	0.95
$r = 600$	0.169	0.96	0.107	0.97	0.149	0.93
$r = 800$	0.148	0.95	0.090	0.95	0.129	0.94
$r = 900$	0.139	0.96	0.083	0.97	0.119	0.95

r increases, length of confidence interval decreases. All of these confirm that the proposed asymptotic variance-covariance formula in (4.12) works well.

5.2 Real Case Studies

Example 3. Well-calibrated traffic flow models are of great help in solving road congestion problems. We apply the proposed method to calibrate the following dual-regime

modified Greenshields traffic flow model (Hou et al., 2013)

$$v_i = \begin{cases} u_f, & 0 < k_i < k_{\mathrm{bp}}, \\ v_0 + (v_f - v_0)\left(1 - \frac{k_i}{k_{\mathrm{jam}}}\right)^{\alpha}, & k_{\mathrm{bp}} < k_i < k_{\mathrm{jam}}, \end{cases} \tag{5.2}$$

where v_i is the vehicle speed, and k_i is the total carriageway density. A total of six parameters affect the shape of the model, which are breakpoint density $k_{bp} \in [0, 20]$, free-flow speed $u_f \in [100, 120]$, speed intercept $v_f \in [150, 220]$, minimum speed $v_0 \in [0, 10]$, jam density $k_{jam} \in [200, 250]$ and shape parameter $\alpha \in [0, 10]$. This model is widely used to predict and explain the trends that are observed in real freeways traffic flows. The traffic data are collected by the detector at London Orbital Motorway M25/4883A on link 199131002, located near Heathrow Airport. We select 35040 traffic data to estimate the calibration parameters. Details about the data can be found in http://tris.highwaysengland.co.uk/detail/trafficflowdata.

Likewise, comparison of the calculation time for different subsample sizes is shown in Table 5. Since the true values of the calibration parameters are unknown, the difference

Table 5: Calculation time (seconds) v.s. different subsample sizes

Criterion	$r = 100$	$r = 200$	$r = 400$	$r = 600$	$r = 800$	$r = n = 35040$
uniform	0.153	0.159	0.217	0.321	0.353	3.227
mV	0.476	0.602	0.684	0.716	0.732	3.583
mVc	0.443	0.549	0.573	0.622	0.689	3.352

between the subsamples estimator and the full data estimator is used to compare the performance of different estimators. Accordingly, define the following,

$$\mathrm{RMSE_f} = \frac{1}{T}\sum_{t=1}^{T}\sum_{j=1}^{q}\left[\frac{\breve{\theta}_j^{(t)} - \hat{\theta}_j}{\hat{\theta}_j}\right]^2. \tag{5.3}$$

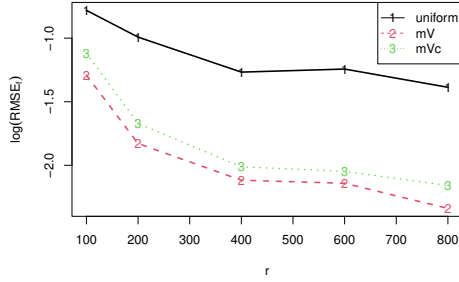The relationship between $\mathrm{RMES_f}$ and r is presented in Figure 5. It shows that the esti-

Figure 5: Accuracy of the proposed estimator for different subsample sizes r and a fixed $r_0 = 22$ based on mV (red), mVc (green) and uniform (black) subsampling methods.

mators based on the mV and mVc criteria outperform the estimator based on the uniform subsampling method.

Next we take α as an example and present its 95% confidence intervals by different subsampling methods. The average lengths of the 95% confidence intervals are presented in Table 6. We do not have a true value in the actual data. As a consequence, the coverage rates are not reported here. So is the next example. For some sample sizes, the confidence

Table 6: Average lengths of 95% confidence intervals for α.

Criterion	$r = 100$	$r = 200$	$r = 400$	$r = 600$	$r = 800$
uniform	11.364	7.761	5.259	4.561	3.950
mV	3.623	2.460	2.263	2.250	1.920
mVc	3.765	2.687	2.106	1.894	1.470

interval lengths obtained by the mV subsampling method are longer than that obtained by the mVc subsampling method. It is acceptable as the optimal subsampling probabilities based on mV is obtained by minimizing $\text{tr}(\mathbf{V})$, that is, minimizing the sum of variance of parameters. In summary, better statistical inference effect can be achieved by the mV and mVc based subsampling methods rather than the uniform based subsampling methods.

29

Example 4. In this example, we consider the calibration of the expensive VarKarst-R model (Hartmann et al., 2015), which is a large-scale simulation model to assess karstic groundwater recharge. The model is a function of precipitation and potential evapotranspiration and its output is karst recharge and actual evapotranspiration. It contains four calibration parameters, which are variability constant $a \in [3, 5]$, mean epikarst storage coefficient $K_{epi} \in [25, 30]$, mean soil storage capacity $V_{soil} \in [530, 545]$, and mean epikarst storage capacity $V_{epi} \in [400, 430]$. A well-calibrated model can help to improve karst water budgets, which inform decisions on drinking water supply and flood risk management. We select 1488 physical observations from December 20, 2003 to January 15, 2008, which is available at https://github.com/KarstHub/VarKarst-R-2015.

Comparison of the calculation time for different subsample sizes is shown in Table 7. The RMSE$_f$s with a fixed $r_0 = 28$ and different subsample sizes are shown in Figure 6.

Table 7: Calculation time (seconds) v.s. different subsample sizes

Criterion	$r = 300$	$r = 400$	$r = 500$	$r = 600$	$r = 800$	$r = n = 1488$
uniform	30.452	43.346	47.677	48.108	64.320	89.244
mV	31.776	48.869	49.411	56.166	66.198	94.782
mVc	31.143	46.470	48.267	53.722	65.862	92.562

Obviously, the estimator based on the mV and mVc criteria works better than that based on the uniform subsampling method. It is worth noting that although the full sample size n is not particularly large in this example, predicting the output of the highly expensive VarKarst-R model at n physical observations points is very time-consuming. The results of this example demonstrate that the proposed estimators using subsamples can approximate the full data estimates very well. It greatly saves the prediction time of the computer model as well as the computational time of the estimation for the calibration parameters.
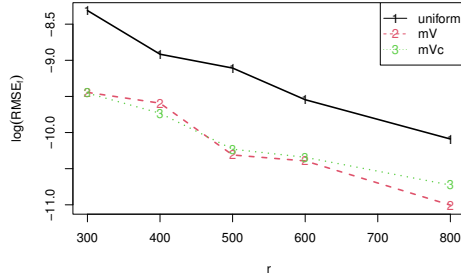
Figure 6: Accuracy of the proposed estimator for different subsample sizes r and a fixed $r_0 = 28$ based on mV (red), mVc (green) and uniform (black) subsampling methods.

Now we construct 95% confidence intervals for a. Table 8 gives the results. Same as the previous example, coverage rates are not shown here also. We can see that the mV and

Table 8: Average lengths of 95% confidence intervals for a.

Criterion	$r = 300$	$r = 400$	$r = 500$	$r = 600$	$r = 800$
uniform	1.019	0.972	0.856	0.685	0.410
mV	0.586	0.511	0.483	0.397	0.308
mVc	0.692	0.513	0.360	0.335	0.324

mVc based subsampling methods are still better than the uniform subsampling method by comparison.

6   Discussion

In this paper, we have proposed a fast calibration method with the subsamples generated by an optimal Poisson subsampling method. The consistency and asymptotic normality of the subsample-based estimators have been established. We have implemented numerical simulations and real case studies to investigate their performance. It turns out that our

proposed method is effective and can extract more useful information than the uniform sampling method.

In this work, we assume that the predictor $\hat{y}^s(\cdot, \cdot)$ for the computer outputs is accurate. However, for non-smooth, extremely expensive computer models, it is difficult to build accurate surrogate models with limited computer experiments. In these cases, the consistency of the OLS calibration will lose. To deal with this problem, an estimator for the calibration parameter that takes into account the uncertainties of the surrogate model is needed. We leave this part for later discussion.

SUPPLEMENTARY MATERIAL

A   Technique proofs

A.1   Proof of Theorem 1

Since $\hat{\boldsymbol{\theta}} - \boldsymbol{\theta}^*$ converges to a normal distribution with mean zero, it is sufficient to prove that conditional on $\mathcal{D}_n$ in probability, there is

$$\tilde{\boldsymbol{\Sigma}}^{-\frac{1}{2}}(\tilde{\boldsymbol{\theta}} - \hat{\boldsymbol{\theta}}) \to N(\mathbf{0}, \mathbf{I}_q) \tag{A.1}$$

in distribution. Here, $\mathbf{I}_q$ is the identity matrix of size q.

Denote $\boldsymbol{a} = (a_1, \ldots, a_n)^T$, with $a_i = 1$ if and only if the i-th data point $(\boldsymbol{x}_i, y_i^p)$ is included in the subsamples. It can be easily seen that a_i follows from Binomial distribution $B(1, \pi_i)$, $i = 1, 2, \ldots, n$. Then there is $\mathrm{E}(a_i) = \pi_i$ and $\mathrm{Var}(a_i) = \pi_i(1 - \pi_i)$.

Here we first prove the consistency of $\tilde{\boldsymbol{\theta}}$. From the definitions of $\tilde{\boldsymbol{\theta}}$ and $\hat{\boldsymbol{\theta}}$, it suffices to prove that $l^*(\boldsymbol{\theta})$ converges to $l(\boldsymbol{\theta})$ uniformly with respect to $\boldsymbol{\theta}$ in conditional probability.

According to the sampling theory, the equation (3.2) can be represented by

$$l^*(\boldsymbol{\theta}) = \frac{1}{n} \sum_{i=1}^{n} a_i \frac{1}{\pi_i} \left[y_i^p - \hat{y}^s(\boldsymbol{x}_i, \boldsymbol{\theta}) \right]^2 .$$

Now, we focus on the conditional expectation and the conditional variance of $l^*(\boldsymbol{\theta}) - l(\boldsymbol{\theta})$.

- The conditional expectation of $l^*(\boldsymbol{\theta})$ is

$$\mathrm{E}_{\boldsymbol{a}}[l^*(\boldsymbol{\theta})|\mathcal{D}_n] = \frac{1}{n} \sum_{i=1}^{n} \left[y_i^p - \hat{y}^s(\boldsymbol{x}_i, \boldsymbol{\theta}) \right]^2 = l(\boldsymbol{\theta}).$$

That is,

$$\mathrm{E}_{\boldsymbol{a}} \left[l^*(\boldsymbol{\theta}) - l(\boldsymbol{\theta})|\mathcal{D}_n \right] = 0. \tag{A.2}$$

- By some elementary calculations, the conditional variance of $l^*(\boldsymbol{\theta}) - l(\boldsymbol{\theta})$ is

$$\begin{aligned}
\mathrm{Var}_{\boldsymbol{a}} \left[l^*(\boldsymbol{\theta}) - l(\boldsymbol{\theta})|\mathcal{D}_n \right] &= \mathrm{Var}_{\boldsymbol{a}} \left\{ \frac{1}{n} \sum_{i=1}^{n} (\frac{a_i}{\pi_i} - 1) \left[y_i^p - \hat{y}^s(\boldsymbol{x}_i, \boldsymbol{\theta}) \right]^2 |\mathcal{D}_n \right\} \\
&= \frac{1}{n^2} \sum_{i=1}^{n} \frac{1 - \pi_i}{\pi_i} \left[y_i^p - \hat{y}^s(\boldsymbol{x}_i, \boldsymbol{\theta}) \right]^4 \tag{A.3} \\
&\leq O_p(\frac{1}{r} + \frac{1}{n}) \frac{1}{n} \sum_{i=1}^{n} \left[y_i^p - \hat{y}^s(\boldsymbol{x}_i, \boldsymbol{\theta}) \right]^4 ,
\end{aligned}$$

the last inequality is obtained from Assumption (H.8). Note that the following equality holds from Assumption (H.1) and Assumption (H.5)

$$\sup_{\boldsymbol{\theta} \in \Theta} \frac{1}{n} \sum_{i=1}^{n} \left[y_i^p - \hat{y}^s(\boldsymbol{x}_i, \boldsymbol{\theta}) \right]^4 = O_p(1). \tag{A.4}$$

Thus, there is

$$\mathrm{Var}_{\boldsymbol{a}} \left[l^*(\boldsymbol{\theta}) - l(\boldsymbol{\theta})|\mathcal{D}_n \right] \leq O_p(r^{-1}). \tag{A.5}$$

The consistency of $\tilde{\boldsymbol{\theta}}$ can be obtained by combining (A.2) and (A.5).

Next, we prove the asymptotic normality of $\tilde{\boldsymbol{\theta}}$. Define $\dot{l}_j^*(\boldsymbol{\theta})$ as the partial derivative of $l^*(\boldsymbol{\theta})$ with respect to θ_j, $j \in \{1, \ldots, q\}$. The asymptotic normality of $\tilde{\boldsymbol{\theta}}$ can be proved by the Delta method for establishing asymptotic theory for M-estimation (Van der Vaart,

2000). According to the definition of $\tilde{\boldsymbol{\theta}}$, we employ Taylor's theorem (Ferguson, 2017) to expand $\dot{l}_j^*(\tilde{\boldsymbol{\theta}})$ at $\hat{\boldsymbol{\theta}}$, that is,

$$0 = \dot{l}_j^*(\tilde{\boldsymbol{\theta}}) = \dot{l}_j^*(\hat{\boldsymbol{\theta}}) + \frac{\partial \dot{l}_j^*(\hat{\boldsymbol{\theta}})}{\partial \boldsymbol{\theta}}(\tilde{\boldsymbol{\theta}} - \hat{\boldsymbol{\theta}}) + R_j, \tag{A.6}$$

where $R_j = (\tilde{\boldsymbol{\theta}} - \hat{\boldsymbol{\theta}})^T \int_0^1 \int_0^1 \frac{\partial^2 \dot{l}_j^*(\hat{\boldsymbol{\theta}} + (\tilde{\boldsymbol{\theta}} - \hat{\boldsymbol{\theta}})uv)}{\partial \boldsymbol{\theta} \partial \boldsymbol{\theta}^T} v \, du \, dv (\tilde{\boldsymbol{\theta}} - \hat{\boldsymbol{\theta}})$.

- First, we consider $\dot{l}_j^*(\hat{\boldsymbol{\theta}})$. Recall that $l^*(\boldsymbol{\theta}) = \frac{1}{n} \sum_{i=1}^r \frac{1}{\pi_i} [y^p(\boldsymbol{x}_i^*) - \hat{y}^s(\boldsymbol{x}_i^*, \boldsymbol{\theta})]^2$. It is obvious that, $\dot{l}_j^*(\hat{\boldsymbol{\theta}})$ can be represented by

$$\dot{l}_j^*(\hat{\boldsymbol{\theta}}) = \frac{2}{n} \sum_{i=1}^n \frac{a_i}{\pi_i} \left[\hat{y}^s(\boldsymbol{x}_i, \hat{\boldsymbol{\theta}}) - y_i^p \right] \frac{\partial \hat{y}^s(\boldsymbol{x}_i, \hat{\boldsymbol{\theta}})}{\partial \theta_j} := \sum_{i=1}^n \eta_i.$$

To find the distribution of $\dot{l}_j^*(\hat{\boldsymbol{\theta}})$, the Lindeberg-Feller condition (Van der Vaart, 2000) is verified as follows. For every constant $\epsilon > 0$,

$$\begin{aligned}
&\sum_{i=1}^n \mathrm{E}_{\boldsymbol{a}} \left[|\eta_i|^2 \, I(|\eta_i| > \epsilon) | \mathcal{D}_n \right] \\
&\leq \frac{1}{\epsilon} \sum_{i=1}^n \mathrm{E}_{\boldsymbol{a}} (|\eta_i|^3 | \mathcal{D}_n) \\
&= \frac{1}{\epsilon} \sum_{i=1}^n \mathrm{E}_{\boldsymbol{a}} \left[\frac{8 a_i^3}{n^3 \pi_i^3} \left| \hat{y}^s(\boldsymbol{x}_i, \hat{\boldsymbol{\theta}}) - y_i^p \right|^3 \left| \frac{\partial \hat{y}^s(\boldsymbol{x}_i, \hat{\boldsymbol{\theta}})}{\partial \theta_j} \right|^3 | \mathcal{D}_n \right] \\
&\leq \frac{1}{\epsilon} \left[\max_{i=1,2,\dots,n} (n \pi_i)^{-2} \right] \frac{1}{n} \sum_{i=1}^n \left| \hat{y}^s(\boldsymbol{x}_i, \hat{\boldsymbol{\theta}}) - y_i^p \right|^3 \left| \frac{\partial \hat{y}^s(\boldsymbol{x}_i, \hat{\boldsymbol{\theta}})}{\partial \theta_j} \right|^3.
\end{aligned} \tag{A.7}$$

By Assumptions (H.5) - (H.6), and the Hölder inequality (Schilling, 2017), we have that

$$\frac{1}{n} \sum_{i=1}^n \left| \hat{y}^s(\boldsymbol{x}_i, \hat{\boldsymbol{\theta}}) - y_i^p \right|^3 \left| \frac{\partial y^s(\boldsymbol{x}_i, \hat{\boldsymbol{\theta}})}{\partial \theta_j} \right|^3 = O_p(1). \tag{A.8}$$

By combining (A.7), (A.8), and Assumption (H.8), we obtain

$$\sum_{i=1}^n \mathrm{E}_{\boldsymbol{a}} \left[|\eta_i|^2 \, I(|\eta_i| > \epsilon) | \mathcal{D}_n \right] \leq \frac{1}{\epsilon} O_p(\frac{1}{r^2}) O_p(1) = o_p(1).$$

Thus, by the Lindeberg-Feller central limit theorem (Van der Vaart, 2000), it can be concluded that as $n \to \infty$ and $r \to \infty$, conditional on $\mathcal{D}_n$,

$$\dot{l}_j^*(\hat{\boldsymbol{\theta}}) | \mathcal{D}_n \sim N \left(\mathrm{E}_{\boldsymbol{a}}[\dot{l}_j^*(\hat{\boldsymbol{\theta}}) | \mathcal{D}_n], \mathrm{Var}_{\boldsymbol{a}}[\dot{l}_j^*(\hat{\boldsymbol{\theta}}) | \mathcal{D}_n] \right). \tag{A.9}$$

By some simple calculations, the conditional expectation of $\dot{l}_j^*(\hat{\boldsymbol{\theta}})$ is

$$\mathrm{E}_{\boldsymbol{a}}\left[\dot{l}_j^*(\hat{\boldsymbol{\theta}})|\mathcal{D}_n\right] = \frac{2}{n}\sum_{i=1}^{n}\left[\hat{y}^s(\boldsymbol{x}_i,\hat{\boldsymbol{\theta}}) - y_i^p\right]\frac{\partial\hat{y}^s(\boldsymbol{x}_i,\hat{\boldsymbol{\theta}})}{\partial\theta_j},$$

and the conditional variance of $\dot{l}_j^*(\hat{\boldsymbol{\theta}})$ can be evaluated by

$$\mathrm{Var}_{\boldsymbol{a}}\left[\dot{l}_j^*(\hat{\boldsymbol{\theta}})|\mathcal{D}_n\right] = \frac{4}{n^2}\sum_{i=1}^{n}\frac{1-\pi_i}{\pi_i}\left\{\left[\hat{y}^s(\boldsymbol{x}_i,\hat{\boldsymbol{\theta}}) - y^p(\boldsymbol{x}_i)\right]\frac{\partial\hat{y}^s(\boldsymbol{x}_i,\hat{\boldsymbol{\theta}})}{\partial\theta_j}\right\}^2 := \tilde{\mathbf{V}}_j,$$

so it shows that $\dot{l}_j^*(\hat{\boldsymbol{\theta}}) = O_{p|\mathcal{D}_n}(r^{-1/2})$.

According to the define of $\hat{\boldsymbol{\theta}}$ (2.4), we have that $\mathrm{E}_{\boldsymbol{a}}[\dot{l}_j^*(\hat{\boldsymbol{\theta}})|\mathcal{D}_n] = 0$. By plugging the conditional expectation and the conditional variance of $\dot{l}_j^*(\hat{\boldsymbol{\theta}})$ into (A.9), we have that as $n \to \infty$ and $r \to \infty$, conditional on $\mathcal{D}_n$,

$$\dot{l}_j^*(\hat{\boldsymbol{\theta}}) \to N(0, \tilde{\mathbf{V}}_j) \tag{A.10}$$

in distribution.

- Next, we consider $\frac{\partial\dot{l}_j^*(\hat{\boldsymbol{\theta}})}{\partial\boldsymbol{\theta}^T}$, which can be written as

$$\frac{\partial\dot{l}_j^*(\hat{\boldsymbol{\theta}})}{\partial\boldsymbol{\theta}^T} = \frac{1}{n}\frac{\partial^2\sum_{i=1}^{n}\frac{a_i}{\pi_i}\left[y_i^p - \hat{y}^s(\boldsymbol{x}_i,\hat{\boldsymbol{\theta}})\right]^2}{\partial\boldsymbol{\theta}^T\partial\theta_j}.$$

By the Lebesgue's dominated convergence theorem, the conditional expectation of $\frac{\partial\dot{l}_j^*(\hat{\boldsymbol{\theta}})}{\partial\boldsymbol{\theta}^T}$ can be represented by

$$\mathrm{E}_{\boldsymbol{a}}\left[\frac{\partial\dot{l}_j^*(\hat{\boldsymbol{\theta}})}{\partial\boldsymbol{\theta}^T}\right] = \frac{1}{n}\sum_{i=1}^{n}\frac{\partial^2\left[y_i^p - \hat{y}^s(\boldsymbol{x}_i,\hat{\boldsymbol{\theta}})\right]^2}{\partial\boldsymbol{\theta}^T\partial\theta_j},$$

and the conditional variance of $\frac{\partial\dot{l}_j^*(\hat{\boldsymbol{\theta}})}{\partial\boldsymbol{\theta}^T}$ is

$$\mathrm{Var}_{\boldsymbol{a}}\left[\frac{\partial\dot{l}_j^*(\hat{\boldsymbol{\theta}})}{\partial\boldsymbol{\theta}^T}\right] = \frac{1}{n^2}\sum_{i=1}^{n}\frac{1-\pi_i}{\pi_i}\frac{\partial^2\left[y_i^p - \hat{y}^s(\boldsymbol{x}_i,\hat{\boldsymbol{\theta}})\right]^2}{\partial\boldsymbol{\theta}^T\partial\theta_j}$$

By using the similar arguments in proving (A.5), we have that under Assumptions (H.5) – (H.8), $\mathrm{Var}_{\boldsymbol{a}}\left[\frac{\partial\dot{l}_j^*(\hat{\boldsymbol{\theta}})}{\partial\boldsymbol{\theta}^T}\right] = O_p(r^{-1})$. As a result,

$$\frac{\partial\dot{l}_j^*(\hat{\boldsymbol{\theta}})}{\partial\boldsymbol{\theta}^T} = \frac{1}{n}\sum_{i=1}^{n}\frac{\partial^2\left[y_i^p - \hat{y}^s(\boldsymbol{x}_i,\hat{\boldsymbol{\theta}})\right]^2}{\partial\boldsymbol{\theta}^T\partial\theta_j} + O_{p|\mathcal{D}_n}(r^{-1/2}) = \tilde{\mathbf{J}} + O_{p|\mathcal{D}_n}(r^{-1/2}). \tag{A.11}$$

- Third, we bound $\int_0^1 \int_0^1 \frac{\partial^2 \dot{l}_j^*(\hat{\boldsymbol{\theta}} + (\tilde{\boldsymbol{\theta}} - \hat{\boldsymbol{\theta}})uv)}{\partial \boldsymbol{\theta} \partial \boldsymbol{\theta}^T} v du dv$.

Suppose $\boldsymbol{\theta}_0 \in \boldsymbol{\Theta}_0$, next we bound $\frac{\partial^2 \dot{l}_j^*(\boldsymbol{\theta}_0)}{\partial \theta_k \partial \theta_{k'}}$, which can be written as follows

$$\frac{\partial \dot{l}_j^*(\boldsymbol{\theta}_0)}{\partial \theta_k \partial \theta_{k'}} = \frac{1}{n} \frac{\partial^3 \sum_{i=1}^n \frac{a_i}{\pi_i} \left[y_i^p - \hat{y}^s(\boldsymbol{x}_i, \boldsymbol{\theta}_0) \right]^2}{\partial \theta_k \partial \theta_{k'} \partial \theta_j}.$$

Similar with (A.11), $\frac{\partial \dot{l}_j^*(\boldsymbol{\theta}_0)}{\partial \theta_k \partial \theta_{k'}}$ can be bounded by

$$\frac{1}{n} \frac{\partial^3 \sum_{i=1}^n \left[y_i^p - \hat{y}^s(\boldsymbol{x}_i, \boldsymbol{\theta}_0) \right]^2}{\partial \theta_k \partial \theta_{k'} \partial \theta_j} + O_p(r^{-1/2}).$$

Because $\|\tilde{\boldsymbol{\theta}} - \hat{\boldsymbol{\theta}}\| = o_{p|\mathcal{D}_n}(1)$, $\hat{\boldsymbol{\theta}} + (\tilde{\boldsymbol{\theta}} - \hat{\boldsymbol{\theta}})uv \in \boldsymbol{\Theta}_0$, it follows that

$$\int_0^1 \int_0^1 \frac{\partial^2 \dot{l}_j^*(\hat{\boldsymbol{\theta}} + (\tilde{\boldsymbol{\theta}} - \hat{\boldsymbol{\theta}})uv)}{\partial \theta_k \partial \theta_{k'}} v du dv = \int_0^1 \int_0^1 \frac{1}{n} \frac{\partial^3 \sum_{i=1}^n \left[y_i^p - \hat{y}^s(\boldsymbol{x}_i, \boldsymbol{\theta}_0) \right]^2}{\partial \theta_k \partial \theta_{k'} \partial \theta_j} v du dv + O_p(r^{-\frac{1}{2}})$$

Because $\frac{1}{n} \frac{\partial^3 \sum_{i=1}^n \left[y_i^p - \hat{y}^s(\boldsymbol{x}_i, \boldsymbol{\theta}_0) \right]^2}{\partial \theta_k \partial \theta_{k'} \partial \theta_j} = O_p(1)$, we have

$$\int_0^1 \int_0^1 \frac{\partial^2 \dot{l}_j^*(\hat{\boldsymbol{\theta}} + (\tilde{\boldsymbol{\theta}} - \hat{\boldsymbol{\theta}})uv)}{\partial \theta_k \partial \theta_{k'}} v du dv = O_p(1). \tag{A.12}$$

By plugging (A.10), (A.11), (A.12) into (A.6), there is

$$\tilde{\boldsymbol{\Sigma}}^{-1/2}(\tilde{\boldsymbol{\theta}} - \hat{\boldsymbol{\theta}}) = -\tilde{\boldsymbol{\Sigma}}^{-1/2} \left[\frac{\partial \dot{l}^*(\hat{\boldsymbol{\theta}})}{\partial \boldsymbol{\theta}^T} \right]^{-1} \dot{l}^*(\hat{\boldsymbol{\theta}}) + O_p(r^{-1/2})$$

$$= -\tilde{\boldsymbol{\Sigma}}^{-1/2} \tilde{\mathbf{J}}^{-1} \dot{l}^*(\hat{\boldsymbol{\theta}}) - \tilde{\boldsymbol{\Sigma}}^{-1/2} \left\{ \left[\frac{\partial \dot{l}^*(\hat{\boldsymbol{\theta}})}{\partial \boldsymbol{\theta}^T} \right]^{-1} - \tilde{\mathbf{J}}^{-1} \right\} \dot{l}^*(\hat{\boldsymbol{\theta}}) + O_p(r^{-1/2})$$

$$= -\tilde{\boldsymbol{\Sigma}}^{-1/2} \tilde{\mathbf{J}}^{-1} \tilde{\mathbf{V}}^{1/2} \tilde{\mathbf{V}}^{-1/2} \dot{l}^*(\hat{\boldsymbol{\theta}}) + O_p(r^{-1/2}).$$

The desired result follows from the Slutsky's Theorem (Ferguson, 2017) and the fact that

$$\tilde{\boldsymbol{\Sigma}}^{-1/2} \tilde{\mathbf{J}}^{-1} \tilde{\mathbf{V}}^{1/2} (\tilde{\boldsymbol{\Sigma}}^{-1/2} \tilde{\mathbf{J}}^{-1} \tilde{\mathbf{V}}^{1/2})^T = \mathbf{I_q}.$$

A.2 Proof of Theorem 2

The subsampling probabilities can be obtained by minimizing the following objective function:

$$\min \quad \text{tr}\left\{\tilde{\mathbf{J}}^{-1}\frac{4}{n^2}\sum_{i=1}^{n}\frac{1}{\pi_i}\left[y_i^p - \hat{y}^s(\boldsymbol{x}_i, \hat{\boldsymbol{\theta}})\right]^2 \frac{\partial \hat{y}^s(\boldsymbol{x}_i, \hat{\boldsymbol{\theta}})}{\partial \boldsymbol{\theta}^T}\frac{\partial \hat{y}^s(\boldsymbol{x}_i, \hat{\boldsymbol{\theta}})}{\partial \boldsymbol{\theta}}\tilde{\mathbf{J}}^{-1}\right\}$$

$$\text{s.t.} \quad \sum_{i=1}^{n}\pi_i = r, \ 0 \le \pi_i \le 1, \ i = 1, \ldots, n. \tag{A.13}$$

Based on the property of the trace of a product, we have that

$$\text{tr}\left\{\tilde{\mathbf{J}}^{-1}\frac{4}{n^2}\sum_{i=1}^{n}\frac{1}{\pi_i}\left[y_i^p - \hat{y}^s(\boldsymbol{x}_i, \hat{\boldsymbol{\theta}})\right]^2 \frac{\partial \hat{y}^s(\boldsymbol{x}_i, \hat{\boldsymbol{\theta}})}{\partial \boldsymbol{\theta}^T}\frac{\partial \hat{y}^s(\boldsymbol{x}_i, \hat{\boldsymbol{\theta}})}{\partial \boldsymbol{\theta}}\tilde{\mathbf{J}}^{-1}\right\}$$

$$= \frac{4}{n^2}\sum_{i=1}^{n}\frac{1}{\pi_i}\left[y_i^p - \hat{y}^s(\boldsymbol{x}_i, \hat{\boldsymbol{\theta}})\right]^2 \frac{\partial \hat{y}^s(\boldsymbol{x}_i, \hat{\boldsymbol{\theta}})}{\partial \boldsymbol{\theta}}\tilde{\mathbf{J}}^{-2}\frac{\partial \hat{y}^s(\boldsymbol{x}_i, \hat{\boldsymbol{\theta}})}{\partial \boldsymbol{\theta}^T} \tag{A.14}$$

$$= \frac{4}{n^2}\left(\frac{1}{r}\sum_{i=1}^{n}\pi_i\right)\sum_{i=1}^{n}\frac{1}{\pi_i}\left[y_i^p - \hat{y}^s(\boldsymbol{x}_i, \hat{\boldsymbol{\theta}})\right]^2 \frac{\partial \hat{y}^s(\boldsymbol{x}_i, \hat{\boldsymbol{\theta}})}{\partial \boldsymbol{\theta}}\tilde{\mathbf{J}}^{-2}\frac{\partial \hat{y}^s(\boldsymbol{x}_i, \hat{\boldsymbol{\theta}})}{\partial \boldsymbol{\theta}^T},$$

the last equality is due to the fact that $\sum_{i=1}^{n}\pi_i = r$.

Define $h_i^{mV} = \left|y_i^p - \hat{y}^s(\boldsymbol{x}_i, \hat{\boldsymbol{\theta}})\right|\left[\frac{\partial \hat{y}^s(\boldsymbol{x}_i, \hat{\boldsymbol{\theta}})}{\partial \boldsymbol{\theta}}\tilde{\mathbf{J}}^{-2}\frac{\partial \hat{y}^s(\boldsymbol{x}_i, \hat{\boldsymbol{\theta}})}{\partial \boldsymbol{\theta}^T}\right]^{1/2}, i = 1, \ldots, n.$ Without losing generality, we assume $h_1^{mV} \le h_2^{mV} \le \ldots \le h_n^{mV}$. (A.14) can continue to be represented by

$$\text{tr}\left\{\tilde{\mathbf{J}}^{-1}\frac{4}{n^2}\sum_{i=1}^{n}\frac{1}{\pi_i}\left[y_i^p - \hat{y}^s(\boldsymbol{x}_i, \hat{\boldsymbol{\theta}})\right]^2 \frac{\partial \hat{y}^s(\boldsymbol{x}_i, \hat{\boldsymbol{\theta}})}{\partial \boldsymbol{\theta}^T}\frac{\partial \hat{y}^s(\boldsymbol{x}_i, \hat{\boldsymbol{\theta}})}{\partial \boldsymbol{\theta}}\tilde{\mathbf{J}}^{-1}\right\}$$

$$\ge \frac{4}{n^2 r}\left\{\sum_{i=1}^{n}\left|y_i^p - \hat{y}^s(\boldsymbol{x}_i, \hat{\boldsymbol{\theta}})\right|\left[\frac{\partial \hat{y}^s(\boldsymbol{x}_i, \hat{\boldsymbol{\theta}})}{\partial \boldsymbol{\theta}^T}\tilde{\mathbf{J}}^{-2}\frac{\partial \hat{y}^s(\boldsymbol{x}_i, \hat{\boldsymbol{\theta}})}{\partial \boldsymbol{\theta}}\right]^{\frac{1}{2}}\right\}^2$$

$$= \frac{4}{n^2 r}\left(\sum_{i=1}^{n}h_i^{mV}\right)^2,$$

the inequality is from the Cauchy-Schwarz inequality and the equality holds if and only if $\pi_i \propto h_i^{mV}$. Next, we consider the following two cases:

- For $i = 1, \ldots, n$, $\pi_i^{mV} = r\frac{h_i^{mV}}{\sum_{j=1}^{n}h_j^{mV}} \le 1$, then $\left\{\pi_i^{mV}\right\}_{i=1}^{n}$ give the optimal solution.

- If there exists some i such that $r\frac{h_i^{mV}}{\sum_{j=1}^{n}h_j^{mV}} > 1$, and from the definition of k, we

know that the number of such i is k, then the initial minimizing formula (A.13) is transformed into the following problem:

$$\min \quad \mathrm{tr}\left\{\tilde{\mathbf{J}}^{-1}\frac{4}{n^2}\sum_{i=1}^{n-k}\frac{1}{\pi_i}\left[y_i^p - y^s(\boldsymbol{x}_i, \hat{\boldsymbol{\theta}})\right]^2 \frac{\partial y^s(\boldsymbol{x}_i, \hat{\boldsymbol{\theta}})}{\partial \boldsymbol{\theta}}\frac{\partial y^s(\boldsymbol{x}_i, \hat{\boldsymbol{\theta}})}{\partial \boldsymbol{\theta}^T}\tilde{\mathbf{J}}^{-1}\right\}$$

$$s.t. \quad \sum_{i=1}^{n-k}\pi_i = r - k,\, 0 \le \pi_i \le 1,\, i = 1, \ldots, n-k, \tag{A.15}$$

$$\pi_{n-k+1}, \ldots, \pi_n = 1.$$

Similar to (A.14), by applying the Cauchy-Schwarz inequality, it holds that

$$\mathrm{tr}\left\{\tilde{\mathbf{J}}^{-1}\frac{4}{n^2}\sum_{i=1}^{n-k}\frac{1}{\pi_i}\left[y_i^p - y^s(\boldsymbol{x}_i, \hat{\boldsymbol{\theta}})\right]^2 \frac{\partial y^s(\boldsymbol{x}_i, \hat{\boldsymbol{\theta}})}{\partial \boldsymbol{\theta}}\frac{\partial y^s(\boldsymbol{x}_i, \hat{\boldsymbol{\theta}})}{\partial \boldsymbol{\theta}^T}\tilde{\mathbf{J}}^{-1}\right\}$$

$$\ge \frac{4}{n^2(r-k)}\left\{\sum_{i=1}^{n-k}\left|y_i^p - y^s(\boldsymbol{x}_i, \hat{\boldsymbol{\theta}})\right|\left[\frac{\partial y^s(\boldsymbol{x}_i, \hat{\boldsymbol{\theta}})}{\partial \boldsymbol{\theta}^T}\tilde{\mathbf{J}}^{-2}\frac{\partial y^s(\boldsymbol{x}_i, \hat{\boldsymbol{\theta}})}{\partial \boldsymbol{\theta}}\right]^{\frac{1}{2}}\right\}^2 \tag{A.16}$$

$$= \frac{4}{n^2(r-k)}\left(\sum_{i=1}^{n-k}h_i^{mV}\right)^2,$$

the equality in the last inequality holds if and only if $\pi_i \propto h_i^{mV}$.

Suppose there exists M such that

$$\max_{i=1,\ldots,n}\frac{h_i^{mV} \wedge M}{\sum_{j=1}^{n}(h_j^{mV} \wedge M)} = \frac{1}{r} \tag{A.17}$$

and $h_{n-k}^{mV} < M \le h_{n-k+1}^{mV}$. Let $\pi_i^{mV} = r\frac{h_i^{mV}\wedge M}{\sum_{j=1}^{n}(h_j^{mV}\wedge M)}$. Next, we verify that π_i^{mV} is the optimal probability. Combining the fact that $\max_{i=1,\ldots,n}h_i^{mV} \wedge M = M$ and (A.17), there is $\sum_{i=1}^{n-k}h_i^{mV} = (r-k)M$. Thus, $\pi_i^{mV} = (r-k)\frac{h_i^{mV}}{\sum_{j=1}^{n-k}h_j^{mV}} = \frac{h_i^{mV}}{M}, i = 1, \ldots, n-k$ and $\pi_i^{mV} = 1, i = n-k+1, \ldots, n$. From the Cauchy-Schwarz inequality, it is clear that π_i^{mV} is the optimal probability that makes the last equality hold in (A.16).

Now we will prove the existence of M and prove that the range of M is $h_{n-k}^{mV} < M \le h_{n-k+1}^{mV}$. From the definition of k, we have that

$$\frac{(r-k+1)h_{n-k+1}^{mV}}{\sum_{i=1}^{n-k+1}h_i^{mV}} \ge 1 \quad \text{and} \quad \frac{(r-k)h_{n-k}^{mV}}{\sum_{i=1}^{n-k}h_i^{mV}} < 1.$$

Denote $M_1 = h_{n-k+1}^{mV}$, $M_2 = h_{n-k}^{mV}$, then there is

$$\frac{(r-k+1)h_{n-k+1}^{mV} + (k-1)M_1}{\sum_{i=1}^{n-k+1} h_i^{mV} + (k-1)M_1} \geq 1 \quad \text{and} \quad \frac{(r-k)h_{n-k}^{mV} + kM_2}{\sum_{i=1}^{n-k} h_i^{mV} + kM_2} < 1,$$

that is $r\frac{h_i^{mV} \wedge M_1}{\sum_{j=1}^n (h_j^{mV} \wedge M_1)} \geq 1$ and $r\frac{h_i^{mV} \wedge M_2}{\sum_{j=1}^n (h_j^{mV} \wedge M_2)} < 1$. Thus the existence of M and $M_2 <$

$M \leq M_1$ are attributed to the continuity of $\max\limits_{i=1,\dots,n} \frac{h_i^{mV} \wedge M}{\sum_{j=1}^n (h_j^{mV} \wedge M)}$.

Otherwise, $\forall \, h_n^{mV} \geq M' > M$, $M' \wedge h_n^{mV} \geq M \wedge h_n^{mV}$, and $\frac{M'}{M} \sum_{i=1}^n h_i^{mV} \wedge M \geq$

$\sum_{i=1}^n h_i^{mV} \wedge M'$, so $\frac{h_n^{mV} \wedge M}{\sum_{j=1}^n (h_j^{mV} \wedge M)}$ is nondecreasing on $M \in (h_1^{mV}, h_n^{mV})$. Therefore

$$\max_{i=1,\dots,n} \frac{h_i^{mV} \wedge M}{\sum_{j=1}^n (h_j^{mV} \wedge M)} = \frac{1}{r}.$$

It indicates that $h_{n-k}^{mV} < M \leq h_{n-k+1}^{mV}$, the proof is completed.

A.3 Proof of Theorem 3

The proof is similar to the proof to Theorem 2, so we ignore details.

A.4 Proof of Theorem 4

Since $\breve{\pi}_i^w \geq \rho r/n$, we have $\max\limits_{i=1,\dots,n} (n\pi_i)^{-1} = O_p(r^{-1})$, Theorem 1 indicates Theorem 4.

A.5 Proof of Theorem 5

Similar with the proof of Theorem 1, it is sufficient to prove that conditional on $\mathcal{D}_n$ in probability,

$$\breve{\boldsymbol{\Sigma}}^{-\frac{1}{2}}(\breve{\boldsymbol{\theta}} - \hat{\boldsymbol{\theta}}) \to N(\mathbf{0}, \mathbf{I}_q) \tag{A.18}$$

in distribution.

Recall that $l_{\hat{\boldsymbol{\theta}}_0}^*(\boldsymbol{\theta}) = \frac{1}{n} \sum_{i=1}^r \frac{1}{\breve{\pi}_i^w \wedge 1} [y^p(\boldsymbol{x}_i^*) - \hat{y}^s(\boldsymbol{x}_i^*, \boldsymbol{\theta})]^2$. The asymptotic normality of $\breve{\boldsymbol{\theta}}$ can be proved by the Delta method for establishing asymptotic theory for M-estimation

(Van der Vaart, 2000). According to the definition of $\breve{\boldsymbol{\theta}}$, we use Taylor's theorem (Ferguson, 2017) to expand $\frac{\partial l^*_{\tilde{\boldsymbol{\theta}}_0}(\breve{\boldsymbol{\theta}})}{\partial \theta_j}$ at $\hat{\boldsymbol{\theta}}$, that is,

$$0 = \frac{\partial l^*_{\tilde{\boldsymbol{\theta}}_0}(\breve{\boldsymbol{\theta}})}{\partial \theta_j} = \frac{\partial l^*_{\tilde{\boldsymbol{\theta}}_0}(\hat{\boldsymbol{\theta}})}{\partial \theta_j} + \frac{\partial^2 l^*_{\tilde{\boldsymbol{\theta}}_0}(\hat{\boldsymbol{\theta}})}{\partial \boldsymbol{\theta} \partial \theta_j}(\breve{\boldsymbol{\theta}} - \hat{\boldsymbol{\theta}}) + R_j, \tag{A.19}$$

where $R_j = (\breve{\boldsymbol{\theta}} - \hat{\boldsymbol{\theta}})^T \int_0^1 \int_0^1 \frac{\partial^3 l^*_{\tilde{\boldsymbol{\theta}}_0}(\hat{\boldsymbol{\theta}} + (\breve{\boldsymbol{\theta}} - \hat{\boldsymbol{\theta}})uv)}{\partial \boldsymbol{\theta} \partial \boldsymbol{\theta}^T \partial \theta_j} v \, du \, dv (\breve{\boldsymbol{\theta}} - \hat{\boldsymbol{\theta}})$.

- First, we consider $\frac{\partial l^*_{\tilde{\boldsymbol{\theta}}_0}(\hat{\boldsymbol{\theta}})}{\partial \theta_j}$, which can be represented by

$$\frac{\partial l^*_{\tilde{\boldsymbol{\theta}}_0}(\hat{\boldsymbol{\theta}})}{\partial \theta_j} = \frac{2}{n} \sum_{i=1}^n a_i \frac{1}{\breve{\pi}^w_i \wedge 1} \left[\hat{y}^s(\boldsymbol{x}_i, \hat{\boldsymbol{\theta}}) - y^p_i\right] \frac{\partial \hat{y}^s(\boldsymbol{x}_i, \hat{\boldsymbol{\theta}})}{\partial \theta_j} := \sum_{i=1}^n \tilde{\eta}_i.$$

To find distribution of $\frac{\partial l^*_{\tilde{\boldsymbol{\theta}}_0}(\hat{\boldsymbol{\theta}})}{\partial \theta_j}$, the Lindeberg-Feller condition (Van der Vaart, 2000) is verified as follows. For every constant $\epsilon > 0$,

$$\sum_{i=1}^n \mathrm{E}_{\boldsymbol{a}} \left[|\tilde{\eta}_i|^2 I(|\tilde{\eta}_i| > \epsilon)|\mathcal{D}_n\right]$$

$$\leq \frac{1}{\epsilon} \sum_{i=1}^n \mathrm{E}_{\boldsymbol{a}} \left[\frac{8a_i^3}{n^3(\breve{\pi}^w_i \wedge 1)^3} \left|\hat{y}^s(\boldsymbol{x}_i, \hat{\boldsymbol{\theta}}) - y^p_i\right|^3 \left|\frac{\partial \hat{y}^s(\boldsymbol{x}_i, \hat{\boldsymbol{\theta}})}{\partial \theta_j}\right|^3 |\mathcal{D}_n\right]$$

$$= o_p(1),$$

the last equality holds for a similar reason to (A.1).

Thus, by the Lindeberg-Feller central limit theorem (Van der Vaart, 2000), it can be concluded that as $n \to \infty$ and $r \to \infty$, conditional on $\mathcal{D}_n$,

$$\frac{\partial l^*_{\tilde{\boldsymbol{\theta}}_0}(\hat{\boldsymbol{\theta}})}{\partial \theta_j} \to N\left(\mathrm{E}_{\boldsymbol{a}}\left[\frac{\partial l^*_{\tilde{\boldsymbol{\theta}}_0}(\hat{\boldsymbol{\theta}})}{\partial \theta_j}|\mathcal{D}_n\right], \mathrm{Var}_{\boldsymbol{a}}\left[\frac{\partial l^*_{\tilde{\boldsymbol{\theta}}_0}(\hat{\boldsymbol{\theta}})}{\partial \theta_j}|\mathcal{D}_n\right]\right) \tag{A.20}$$

in distribution.

By some simple calculations, the conditional expectation of $\frac{\partial l^*_{\tilde{\boldsymbol{\theta}}_0}(\hat{\boldsymbol{\theta}})}{\partial \theta_j}$ is

$$\mathrm{E}_{\boldsymbol{a}}\left[\frac{\partial l^*_{\tilde{\boldsymbol{\theta}}_0}(\hat{\boldsymbol{\theta}})}{\partial \theta_j}|\mathcal{D}_n\right] = \frac{2}{n} \sum_{i=1}^n \left[\hat{y}^s(\boldsymbol{x}_i, \hat{\boldsymbol{\theta}}) - y^p_i\right] \frac{\partial \hat{y}^s(\boldsymbol{x}_i, \hat{\boldsymbol{\theta}})}{\partial \theta_j},$$

and the conditional variance of $\frac{\partial l^*_{\tilde{\boldsymbol{\theta}}_0}(\hat{\boldsymbol{\theta}})}{\partial \theta_j}$ can be evaluated by

$$\mathrm{Var}_{\boldsymbol{a}}\left[\frac{\partial l^*_{\tilde{\boldsymbol{\theta}}_0}(\hat{\boldsymbol{\theta}})}{\partial \theta_j}|\mathcal{D}_n\right] = \frac{4}{n^2} \sum_{i=1}^n \frac{1 - \breve{\pi}^w_i \wedge 1}{\breve{\pi}^w_i \wedge 1} \left\{\left[\hat{y}^s(\boldsymbol{x}_i, \hat{\boldsymbol{\theta}}) - y^p_i\right] \frac{\partial \hat{y}^s(\boldsymbol{x}_i, \hat{\boldsymbol{\theta}})}{\partial \theta_j}\right\}^2 := \breve{\mathbf{V}}^w_j.$$

According to the define of $\hat{\boldsymbol{\theta}}$, we have that $\mathrm{E}_{\boldsymbol{a}}\left[\frac{\partial l_{\tilde{\boldsymbol{\theta}}_0}^*(\hat{\boldsymbol{\theta}})}{\partial \theta_j}|\mathcal{D}_n\right] = 0$. By plugging the conditional expectation and the conditional variance of $\frac{\partial l_{\tilde{\boldsymbol{\theta}}_0}^*(\hat{\boldsymbol{\theta}})}{\partial \theta_j}$ into (A.20), we have that as $n \to \infty$ and $r \to \infty$, conditional on $\mathcal{D}_n$,

$$\frac{\partial l_{\tilde{\boldsymbol{\theta}}_0}^*(\hat{\boldsymbol{\theta}})}{\partial \theta_j} \to N(0, \breve{\mathbf{V}}_j^w). \tag{A.21}$$

in distribution.

Now, we discuss the distance between $\breve{\mathbf{V}}^w$ and $\tilde{\mathbf{V}}^w$. Let $\|\boldsymbol{A}\|_s$ be the spectral norm of a vector or matrix $\boldsymbol{A}$, there is

$$
\begin{aligned}
&\left\|\breve{\mathbf{V}}^w - \tilde{\mathbf{V}}^w\right\|_s \\
&= \left\|\frac{4}{n^2} \sum_{i=1}^n \frac{1}{\pi_i^w \wedge 1}\left(\frac{\pi_i^w \wedge 1}{\breve{\pi}_i^w \wedge 1} - 1\right)\left[\hat{y}^s(\boldsymbol{x}_i, \hat{\boldsymbol{\theta}}) - y_i^p\right]^2 \frac{\partial \hat{y}^s(\boldsymbol{x}_i, \hat{\boldsymbol{\theta}})}{\partial \boldsymbol{\theta}^T} \frac{\partial \hat{y}^s(\boldsymbol{x}_i, \hat{\boldsymbol{\theta}})}{\partial \boldsymbol{\theta}}\right\|_s \\
&\leq \frac{4}{n^2} \sum_{i=1}^n \frac{1}{\pi_i^w \wedge 1}\left|\frac{\pi_i^w \wedge 1}{\breve{\pi}_i^w \wedge 1} - 1\right|\left[\hat{y}^s(\boldsymbol{x}_i, \hat{\boldsymbol{\theta}}) - y_i^p\right]^2 \frac{\partial \hat{y}^s(\boldsymbol{x}_i, \hat{\boldsymbol{\theta}})}{\partial \boldsymbol{\theta}} \frac{\partial \hat{y}^s(\boldsymbol{x}_i, \hat{\boldsymbol{\theta}})}{\partial \boldsymbol{\theta}^T} \\
&\leq \left(\max_{i=1,\ldots,n} \frac{1}{n\pi_i^w}\right) \frac{4}{n} \sum_{i=1}^n \left|\frac{\pi_i^w \wedge 1}{\breve{\pi}_i^w \wedge 1} - 1\right|\left[\hat{y}^s(\boldsymbol{x}_i, \hat{\boldsymbol{\theta}}) - y_i^p\right]^2 \frac{\partial \hat{y}^s(\boldsymbol{x}_i, \hat{\boldsymbol{\theta}})}{\partial \boldsymbol{\theta}} \frac{\partial \hat{y}^s(\boldsymbol{x}_i, \hat{\boldsymbol{\theta}})}{\partial \boldsymbol{\theta}^T} \\
&\leq \frac{1}{\rho r} \frac{4}{n} \sum_{i=1}^n \left|\frac{\pi_i^w \wedge 1}{\breve{\pi}_i^w \wedge 1} - 1\right|\left[\hat{y}^s(\boldsymbol{x}_i, \hat{\boldsymbol{\theta}}) - y_i^p\right]^2 \frac{\partial \hat{y}^s(\boldsymbol{x}_i, \hat{\boldsymbol{\theta}})}{\partial \boldsymbol{\theta}} \frac{\partial \hat{y}^s(\boldsymbol{x}_i, \hat{\boldsymbol{\theta}})}{\partial \boldsymbol{\theta}^T},
\end{aligned}
$$

where the last inequality holds from (4.5). We consider the case under the mV criterion, and the same goes for the mVc criterion. Let $h_0^{mV}(\boldsymbol{x}_i)$ be the value of h_i^{mV} with $\hat{\boldsymbol{\theta}}$ replaced by the pilot estimator $\tilde{\boldsymbol{\theta}}_0$. Since

$$
\left|\frac{\pi_i^w \wedge 1}{\breve{\pi}_i^w \wedge 1} - 1\right| \leq \left|\frac{\pi_i^w - \breve{\pi}_i^w}{\breve{\pi}_i^w}\right| \leq (1-\rho)\left|\frac{\frac{h_0^{mV}(\boldsymbol{x}_i)}{\sum_{i=1}^n h_0^{mV}(\boldsymbol{x}_i)} - \frac{h_i^{mV}}{\sum_{i=1}^n h_i^{mV}}}{\rho r \frac{1}{n}}\right|
$$

$$
\leq \frac{\left|\frac{h_0^{mV}(\boldsymbol{x}_i)}{\sum_{i=1}^n h_0^{mV}(\boldsymbol{x}_i)} - \frac{h_i^{mV}}{\sum_{i=1}^n h_0^{mV}(\boldsymbol{x}_i)}\right| + \left|\frac{h_i^{mV}}{\sum_{i=1}^n h_0^{mV}(\boldsymbol{x}_i)} - \frac{h_i^{mV}}{\sum_{i=1}^n h_i^{mV}}\right|}{\rho r \frac{1}{n}},
$$

by some simple calculations, we have that

$$\frac{1}{n}\sum_{i=1}^{n}\left|\frac{\pi_i^w \wedge 1}{\breve{\pi}_i^w \wedge 1} - 1\right|\left[\hat{y}^s(\boldsymbol{x}_i,\hat{\boldsymbol{\theta}}) - y_i^p\right]^2\frac{\partial\hat{y}^s(\boldsymbol{x}_i,\hat{\boldsymbol{\theta}})}{\partial\boldsymbol{\theta}}\frac{\partial\hat{y}^s(\boldsymbol{x}_i,\hat{\boldsymbol{\theta}})}{\partial\boldsymbol{\theta}^T}$$

$$\leq \frac{\sum_{i=1}^{n}h_i^{mV}}{\sum_{i=1}^{n}h_0^{mV}(\boldsymbol{x}_i)}\sum_{i=1}^{n}\frac{\left[\hat{y}^s(\boldsymbol{x}_i,\hat{\boldsymbol{\theta}}) - y_i^p\right]^2\frac{\partial\hat{y}^s(\boldsymbol{x}_i,\hat{\boldsymbol{\theta}})}{\partial\boldsymbol{\theta}}\frac{\partial\hat{y}^s(\boldsymbol{x}_i,\hat{\boldsymbol{\theta}})}{\partial\boldsymbol{\theta}^T}}{n}\frac{\left|h_0^{mV}(\boldsymbol{x}_i) - h_i^{mV}\right|}{\rho r\frac{1}{n}\sum_{i=1}^{n}h_i^{mV}} \tag{A.22}$$

$$+\left|\frac{\sum_{i=1}^{n}h_i^{mV}}{\sum_{i=1}^{n}h_0^{mV}(\boldsymbol{x}_i)} - 1\right|\sum_{i=1}^{n}\frac{\left[\hat{y}^s(\boldsymbol{x}_i,\hat{\boldsymbol{\theta}}) - y_i^p\right]^2\frac{\partial\hat{y}^s(\boldsymbol{x}_i,\hat{\boldsymbol{\theta}})}{\partial\boldsymbol{\theta}}\frac{\partial\hat{y}^s(\boldsymbol{x}_i,\hat{\boldsymbol{\theta}})}{\partial\boldsymbol{\theta}^T}}{n}\frac{h_i^{mV}}{\rho r\frac{1}{n}\sum_{i=1}^{n}h_i^{mV}}.$$

Write $\frac{\partial\hat{y}^s(\boldsymbol{x}_i,\hat{\boldsymbol{\theta}})}{\partial\boldsymbol{\theta}}\frac{\partial\hat{y}^s(\boldsymbol{x}_i,\hat{\boldsymbol{\theta}})}{\partial\boldsymbol{\theta}^T} = \|\frac{\partial\hat{y}^s(\boldsymbol{x}_i,\hat{\boldsymbol{\theta}})}{\partial\boldsymbol{\theta}^T}\|_E$. Now we bound (A.22). By combining the triangle

inequality and the consistency $\tilde{\boldsymbol{\theta}}_0$, it follows that

$$\left|h_0^{mV}(\boldsymbol{x}_i) - h_i^{mV}\right|$$

$$\leq \left|\hat{y}^s(\boldsymbol{x}_i,\tilde{\boldsymbol{\theta}}_0) - \hat{y}^s(\boldsymbol{x}_i,\hat{\boldsymbol{\theta}})\right|\left[\frac{\partial\hat{y}^s(\boldsymbol{x}_i,\tilde{\boldsymbol{\theta}}_0)}{\partial\boldsymbol{\theta}}\tilde{\mathbf{J}}_0^{-2}\frac{\partial\hat{y}^s(\boldsymbol{x}_i,\tilde{\boldsymbol{\theta}}_0)}{\partial\boldsymbol{\theta}^T}\right]^{\frac{1}{2}}$$

$$+ \left|\hat{y}^s(\boldsymbol{x}_i,\tilde{\boldsymbol{\theta}}_0) - \hat{y}^s(\boldsymbol{x}_i,\hat{\boldsymbol{\theta}})\right|\left[\frac{\partial\hat{y}^s(\boldsymbol{x}_i,\hat{\boldsymbol{\theta}})}{\partial\boldsymbol{\theta}}\tilde{\mathbf{J}}^{-2}\frac{\partial\hat{y}^s(\boldsymbol{x}_i,\hat{\boldsymbol{\theta}})}{\partial\boldsymbol{\theta}^T}\right]^{\frac{1}{2}}.$$

Assumption (H.7) and the consistency of $\tilde{\boldsymbol{\theta}}_0$ indicate that

$$\left|\hat{y}^s(\boldsymbol{x}_i,\hat{\boldsymbol{\theta}}) - \hat{y}^s(\boldsymbol{x}_i,\tilde{\boldsymbol{\theta}}_0)\right| \leq m_1(x_i)\left\|\hat{\boldsymbol{\theta}} - \tilde{\boldsymbol{\theta}}_0\right\|_E = o_p(1).$$

Also, by the consistency of $\tilde{\boldsymbol{\theta}}_0$, we have that $\tilde{\mathbf{J}}_0$ converges to $\tilde{\mathbf{J}}$ in probability. Together

with the fact that $\left[\frac{\partial\hat{y}^s(\boldsymbol{x}_i,\hat{\boldsymbol{\theta}})}{\partial\boldsymbol{\theta}}\tilde{\mathbf{J}}^{-2}\frac{\partial\hat{y}^s(\boldsymbol{x}_i,\hat{\boldsymbol{\theta}})}{\partial\boldsymbol{\theta}^T}\right] \leq \lambda_{\max}(\tilde{\mathbf{J}}^{-1})\left\|\frac{\partial\hat{y}^s(\boldsymbol{x}_i,\hat{\boldsymbol{\theta}})}{\partial\boldsymbol{\theta}^T}\right\|_E$, there is

$$\left|h_0^{mV}(\boldsymbol{x}_i) - h_i^{mV}\right| = o_p(1). \tag{A.23}$$

Thus, there is

$$\frac{1}{n}\sum_{i=1}^{n}h_i^{mV} = \frac{1}{n}\sum_{i=1}^{n}h_0^{mV}(\boldsymbol{x}_i) + o_p(1). \tag{A.24}$$

Because

$$\frac{1}{n}\sum_{i=1}^{n}h_i^{mV} = \frac{1}{n}\sum_{i=1}^{n}\left|y_i^p - \hat{y}^s(\boldsymbol{x}_i,\hat{\boldsymbol{\theta}})\right|\left[\frac{\partial\hat{y}^s(\boldsymbol{x}_i,\hat{\boldsymbol{\theta}})}{\partial\boldsymbol{\theta}}\tilde{\mathbf{J}}^{-2}\frac{\partial\hat{y}^s(\boldsymbol{x}_i,\hat{\boldsymbol{\theta}})}{\partial\boldsymbol{\theta}^T}\right]^{1/2}$$

$$\geq \lambda_{\min}(\tilde{\mathbf{J}}^{-1})\frac{1}{n}\sum_{i=1}^{n}\left|y_i^p - \hat{y}^s(\boldsymbol{x}_i,\hat{\boldsymbol{\theta}})\right|\left\|\frac{\partial\hat{y}^s(\boldsymbol{x}_i,\hat{\boldsymbol{\theta}})}{\partial\boldsymbol{\theta}^T}\right\|_E,$$

and $\frac{1}{n}\sum_{i=1}^n \left[y_i^p - \hat{y}^s(\boldsymbol{x}_i, \hat{\boldsymbol{\theta}}) \right]^2 \left\| \frac{\partial \hat{y}^s(\boldsymbol{x}_i, \hat{\boldsymbol{\theta}})}{\partial \boldsymbol{\theta}^T} \right\|_E^2 = O_p(1)$ from Assumptions (H.5) – (H.6), it follows that

$$\left(\frac{1}{n}\sum_{i=1}^n h_i^{mV} \right)^{-1} = O_p(1). \tag{A.25}$$

By plugging (A.23) – (A.25) into (A.22), there is

$$\left\| \breve{\mathbf{V}}^w - \tilde{\mathbf{V}}^w \right\|_s = o_p(r^{-1}). \tag{A.26}$$

- Next, we consider $\frac{\partial^2 l_{\tilde{\boldsymbol{\theta}}_0}^*(\hat{\boldsymbol{\theta}})}{\partial \boldsymbol{\theta}^T \partial \theta_j}$, which can be written as

$$\frac{\partial^2 l_{\tilde{\boldsymbol{\theta}}_0}^*(\hat{\boldsymbol{\theta}})}{\partial \boldsymbol{\theta}^T \partial \theta_j} = \frac{1}{n} \frac{\partial^2 \sum_{i=1}^n \frac{a_i}{\tilde{\pi}_i^w \wedge 1} \left[y_i^p - \hat{y}^s(\boldsymbol{x}_i, \hat{\boldsymbol{\theta}}) \right]^2}{\partial \boldsymbol{\theta}^T \partial \theta_j}. \tag{A.27}$$

Using the arguments similar to (A.11), (A.27) can be represented by

$$\frac{1}{n} \frac{\partial^2 \sum_{i=1}^n \frac{a_i}{\tilde{\pi}_i^w \wedge 1} \left[y_i^p - \hat{y}^s(\boldsymbol{x}_i, \hat{\boldsymbol{\theta}}) \right]^2}{\partial \boldsymbol{\theta}^T \partial \theta_j} = \frac{1}{n} \sum_{i=1}^n \frac{\partial^2 \left[y_i^p - \hat{y}^s(\boldsymbol{x}_i, \hat{\boldsymbol{\theta}}) \right]^2}{\partial \boldsymbol{\theta}^T \partial \theta_j} + O_p(r^{-\frac{1}{2}}). \tag{A.28}$$

- Third, we bound $\int_0^1 \int_0^1 \frac{\partial^3 l_{\tilde{\boldsymbol{\theta}}_0}^*(\hat{\boldsymbol{\theta}} + (\breve{\boldsymbol{\theta}} - \hat{\boldsymbol{\theta}})uv)}{\partial \boldsymbol{\theta} \partial \boldsymbol{\theta}^T \partial \theta_j} v\, du\, dv$.

Suppose $\boldsymbol{\theta}_0 \in \boldsymbol{\Theta}_0$, next we bound $\frac{\partial^3 l_{\tilde{\boldsymbol{\theta}}_0}^*(\boldsymbol{\theta}_0)}{\partial \theta_k \partial \theta_{k'} \partial \theta_j}$, which can be written as follows

$$\frac{\partial^3 l_{\tilde{\boldsymbol{\theta}}_0}^*(\boldsymbol{\theta}_0)}{\partial \theta_k \partial \theta_{k'} \partial \theta_j} = \frac{1}{n} \frac{\partial^3 \sum_{i=1}^n \frac{a_i}{\tilde{\pi}_i^w \wedge 1} \left[y_i^p - \hat{y}^s(\boldsymbol{x}_i, \boldsymbol{\theta}_0) \right]^2}{\partial \theta_k \partial \theta_{k'} \partial \theta_j}.$$

Similar with (A.11), $\frac{\partial^3 l_{\tilde{\boldsymbol{\theta}}_0}^*(\boldsymbol{\theta}_0)}{\partial \theta_k \partial \theta_{k'} \partial \theta_j}$ can be bounded by

$$\frac{1}{n} \frac{\partial^3 \sum_{i=1}^n \left[y_i^p - \hat{y}^s(\boldsymbol{x}_i, \boldsymbol{\theta}_0) \right]^2}{\partial \theta_k \partial \theta_{k'} \partial \theta_j} + O_p(r^{-1/2}).$$

Because $\|\breve{\boldsymbol{\theta}} - \hat{\boldsymbol{\theta}}\|_E = o_{p|\mathcal{D}_n}(1)$, $\hat{\boldsymbol{\theta}} + (\breve{\boldsymbol{\theta}} - \hat{\boldsymbol{\theta}})uv \in \boldsymbol{\Theta}_0$, similar to (A.12), it follows that

$$\int_0^1 \int_0^1 \frac{\partial^3 l_{\tilde{\boldsymbol{\theta}}_0}^*(\hat{\boldsymbol{\theta}} + (\breve{\boldsymbol{\theta}} - \hat{\boldsymbol{\theta}})uv)}{\partial \theta_k \partial \theta_k' \partial \theta_j} v\, du\, dv = \int_0^1 \int_0^1 \frac{1}{n} \frac{\partial^3 \sum_{i=1}^n \left[y_i^p - \hat{y}^s(\boldsymbol{x}_i, \boldsymbol{\theta}_0) \right]^2}{\partial \theta_k \partial \theta_{k'} \partial \theta_j} v\, du\, dv + O_p(r^{-\frac{1}{2}})$$

$$= O_p(1). \tag{A.29}$$

The desired result can be obtained by plugging (A.21) and (A.26) – (A.29) into (A.19).

References

Ai, M., F. Wang, J. Yu, and H. Zhang (2021). Optimal subsampling for large-scale quantile regression. *Journal of Complexity 62*, 101512.

Ai, M., J. Yu, H. Zhang, and H. Wang (2021). Optimal subsampling algorithms for big data regressions. *Statistica Sinica 31*, 749–772.

Bottou, L. (2010). Large-scale machine learning with stochastic gradient descent. In *Proceedings of COMPSTAT'2010*, pp. 177–186. Springer.

Breidt, F. J. and J. D. Opsomer (2000). Local polynomial regression estimators in survey sampling. *Annals of Statistics*, 1026–1053.

Cai, G. and S. Mahadevan (2017). Model calibration with big data. In *Model Validation and Uncertainty Quantification, Volume 3*, pp. 315–322. Springer.

Chang, K.-L. and S. Guillas (2019). Computer model calibration with large non-stationary spatial outputs: application to the calibration of a climate model. *Journal of the Royal Statistical Society: Series C (Applied Statistics) 68*(1), 51–78.

Ezzat, A. A., A. Pourhabib, and Y. Ding (2018). Sequential design for functional calibration of computer models. *Technometrics 60*(3), 286–296.

Ferguson, T. S. (2017). *A course in large sample theory*. Routledge.

Haaland, B., W. Wang, and V. Maheshwari (2018). A framework for controlling sources of inaccuracy in gaussian process emulation of deterministic computer experiments. *SIAM/ASA Journal on Uncertainty Quantification 6*(2), 497–521.

Hartmann, A., T. Gleeson, R. Rosolem, F. Pianosi, Y. Wada, and T. Wagener (2015). A large-scale simulation model to assess karstic groundwater recharge over europe and the mediterranean. *Geoscientific Model Development 8*(6), 1729–1746.

Hou, T., H. S. Mahmassani, R. M. Alfelor, J. Kim, and M. Saberi (2013). Calibration of traffic flow models under adverse weather and application in mesoscopic network simulation. *Transportation Research Record 2391*(1), 92–104.

Johnson, M. E., L. M. Moore, and D. Ylvisaker (1990). Minimax and maximin distance designs. *Journal of Statistical Planning and Inference 26*(2), 131–148.

Kennedy, M. C. and A. O'Hagan (2001). Bayesian calibration of computer models. *Journal of the Royal Statistical Society: Series B (Statistical Methodology) 63*(3), 425–464.

Krishna, A., V. R. Joseph, S. Ba, W. A. Brenneman, and W. R. Myers (2021). Robust experimental designs for model calibration. *Journal of Quality Technology*, 1–12.

Loeppky, J. L. and S. W. J. Welch (2009). Choosing the sample size of a computer experiment: A practical guide. *Technometrics 51*(4), 366–376.

Ma, P., M. Mahoney, and B. Yu (2014). A statistical perspective on algorithmic leveraging. In *International Conference on Machine Learning*, pp. 91–99. PMLR.

Mahoney, M. W., B. EDU, and B. Yu (2015). A statistical perspective on algorithmic leveraging. *Journal of Machine Learning Research 16*, 861–911.

Plumlee, M. (2017). Bayesian calibration of inexact computer models. *Journal of the American Statistical Association 112*(519), 1274–1285.

Pukelsheim, F. (2006). *Optimal design of experiments*. SIAM.

Santner, T. J., B. J. Williams, and W. I. Notz (2018). *The design and analysis of computer experiments*, Volume 2. Springer.

Schilling, R. L. (2017). *Measures, integrals and martingales.* Cambridge University Press.

Tsai, W.-P., D. Feng, M. Pan, H. Beck, K. Lawson, Y. Yang, J. Liu, and C. Shen (2021). From calibration to parameter learning: Harnessing the scaling effects of big data in geoscientific modeling. *Nature Communications 12*(1), 1–13.

Tuo, R. (2019). Adjustments to computer models via projected kernel calibration. *SIAM/ASA Journal on Uncertainty Quantification 7*(2), 553–578.

Tuo, R. and C. F. J. Wu (2015). Efficient calibration for imperfect computer models. *The Annals of Statistics 43*(6), 2331–2352.

Van der Vaart, A. W. (2000). *Asymptotic statistics*, Volume 3. Cambridge University Press.

Varadhan, R. and P. Gilbert (2010). Bb: An r package for solving a large system of nonlinear equations and for optimizing a high-dimensional nonlinear objective function. *Journal of Statistical Software 32*, 1–26.

Wang, H. and Y. Ma (2021). Optimal subsampling for quantile regression in big data. *Biometrika 108*(1), 99–112.

Wang, H., M. Yang, and J. Stufken (2019). Information-based optimal subdata selection for big data linear regression. *Journal of the American Statistical Association 114*(525), 393–405.

Wang, H., R. Zhu, and P. Ma (2018). Optimal subsampling for large sample logistic regression. *Journal of the American Statistical Association 113*(522), 829–844.

Wong, R. K., C. B. Storlie, and T. C. Lee (2017). A frequentist approach to computer model calibration. *Journal of the Royal Statistical Society: Series B (Statistical Methodology) 79*(2), 635–648.

Xie, F. and Y. Xu (2021). Bayesian projected calibration of computer models. *Journal of the American Statistical Association 116*(536), 1965–1982.

Xiong, S., P. Z. Qian, and C. J. Wu (2013). Sequential design and analysis of high-accuracy and low-accuracy computer codes. *Technometrics 55*(1), 37–46.

Yao, Y. and H. Wang (2019). Optimal subsampling for softmax regression. *Statistical Papers 60*(2), 585–599.

Yu, J., H. Wang, M. Ai, and H. Zhang (2022). Optimal distributed subsampling for maximum quasi-likelihood estimators with massive data. *Journal of the American Statistical Association 117*(537), 265–276.

Zhu, R. (2016). Gradient-based sampling: An adaptive importance sampling for least-squares. *Advances in Neural Information Processing Systems 29*.